AN ABSTRACT OF THE THESIS OF

Rajoana Rojony for the degree of Master of Science in Comparative Health Sciences presented on August 1, 2019.

Title: Quantitative Analysis of *Mycobacterium avium* subsp. *hominissuis* and *Mycobacterium abscessus* subs. *abscessus* Proteome in Response to Antibiotics and During Exposure to Different Environmental Conditions.

Abstract approved:

Lia Danelishvili Luis E. Bermudez

M. avium subsp. *hominissuis* (MAH) and *M. abscessus* subsp. *abscessus* (MAB) both belong to the clinically important non-tuberculous mycobacterial (NTM) group that infect immunocompromised patients with AIDS and individuals with underlining lung conditions such as bronchiectasis or cystic fibrosis. The main challenge of treating MAH and MAB patients is an inability to rapidly kill pathogens with multiple compounds even at the bactericidal concentrations. As a result, MAV requires prolonged treatment for 15 to 18 months and MAB is the multidrug resistant pathogenic NTM that requires treatment for 18-24 month. The need for prolonged therapy for MAH and MAB treatment influences the development of persistent and drug-resistant infections. The reason why several drugs at their bactericidal concentrations take several months to eliminate MAH and MAB infections is unknown. The main goal of our research was to investigate MAH and MAB proteome response under aerobic, anaerobic and biofilm conditions that are encountered in patient lungs and intracellularly with or without bactericidal concentrations of antibiotics. In order to

identify proteome remodeling and metabolic changes enhancing bacterial tolerance during biofilm and anaerobic conditions with or without exposure of bactericidal concentrations of antibiotics, we performed the relative protein quantitative analysis using Tandem Mass Tag Mass Spectrometry sequencing.

We identified proteome remodeling of MAH under aerobic, anaerobic and biofilm conditions in presence or absence of amikacin (4 μg/ml) and clarithromycin (16 μg/ml), and the response was compared. Overall, 4,000 MAH proteins were identified across all experimental group. In both anaerobic and biofilm conditions, MAH upregulates pantothenate and CoA biosynthesis, glycerolipid metabolism, nitrogen metabolism and chloroalkene degradation which are known to be associated with bacterial tolerance in *M. tuberculosis*. In anaerobic and biofilm conditions following drug treatments peptidoglycan biosynthesis, glycerophospholipid metabolism, and protein export pathways were highly upregulated.

We also identified proteome remodeling of MAB under aerobic anaerobic and biofilm conditions in presence or absence of amikacin (32μg/ml) and linezolid (128 μg/ml), and the response was compared. We found glycolysis/gluconeogenesis, citrate cycle (TCA cycle), oxidative phosphorylation, nitrogen metabolism, and glyoxylate and dicarboxylate metabolism pathways expressed exclusively in both anaerobic and biofilm conditions. Following 24h drug treatments in anaerobic and biofilm conditions, the glycerophospholipid metabolism and oxidative phosphorylation are commonly observed.

Cumulatively, our work significantly advances the knowledge on MAH and MAB tolerance mechanism in biofilms and anaerobic conditions, and how they tolerate high concentrations of antibiotics. Current multidrug regimens fail to effectively eliminate MAH and MAB infection and eradicates MAH in only 40% to 60% of individuals, and success rate for MAB treatment is only 25% to 42%. Our study has identified several novel targets that may contribute to the rapid killing of MAH and MAB.

Quantitative Analysis of *Mycobacterium avium* subsp. *hominissuis* and *Mycobacterium abscessus* subs. *abscessus* Proteome in Response to Antibiotics and During Exposure to Different Environmental Conditions

by
Rajoana Rojony

A THESIS

submitted to

Oregon State University

in partial fulfillment of
the requirements for the
degree of

Master of Science

Presented August 1, 2019
Commencement June 2020

Master of Science thesis of Rajoana Rojony presented on August 1, 2019

APPROVED:

Co-Major Professor, representing Comparative Health Sciences

Co-Major Professor, representing Comparative Health Sciences

Dean of the College of Veterinary Medicine

Dean of the Graduate School

I understand that my thesis will become part of the permanent collection of Oregon State University libraries. My signature below authorizes release of my thesis to any reader upon request.

Rajoana Rojony, Author

ACKNOWLEDGEMENTS

First, I am very thankful to Dr. Luiz Bermudez for believing in my potential and giving me the opportunity to conduct research in his laboratory. He provided invaluable guidance throughout this research. His dynamism, vision, sincerity and motivation have deeply inspired me. I am extremely grateful for what he has offered me. I am very grateful to Dr. Lia Danelishvili for her continuous mentorship, friendship, empathy, patience and enthusiasm. Her guidance helped me all the time conducting experiments and writing thesis. I could not have imagined having a better advisor and mentor for my master's study. Besides my two advisor, I would like to thank the rest of my thesis committee members Dr. Taifo Mahmud and Dr.Marit L. Bovbjerg for agreeing to be on my committee and for providing me helpful feedback. I would also like to thank everybody in the Bermudez laboratory for the support, teamwork, conversations, and guidance to help me throughout my journey.

Big thank to my husband for his continuous moral support and encouragement. I dedicate this work to my husband. I will always endeavor to make you proud.

This work was supported by a grant of the Microbiology Foundation of San Francisco.

CONTRIBUTION OF AUTHORS

Chapter 1: Rajoana Rojony wrote the general introduction. Lia Danelishvili and Luiz Bermudez contributed to the editing process.

Chapter 2: Rajoana Rojony designed, performed experiments, analyzed results, and wrote the manuscript. Matthew Martin and Pankaj Jaiswal analyzed proteomic data. Anaamika Campeau, Jacob M. Wozniak and David J. Gonzalez performed proteome sequencing and analyzed results. L. Danelishvili designed and performed experiments, analyzed results, helped to write manuscripts. Luiz Bermudez helped design the experiments, guided the ideas, provided important review of the manuscript.

Chapter 3: Rajoana Rojony designed, performed experiments, analyzed results, and wrote the manuscript. Anaamika Campeau, Jacob M. Wozniak and David J. Gonzalez performed proteome sequencing, analyzed results. L. Danelishvili designed and performed experiments, analyzed results, helped to write manuscripts. Luiz Bermudez helped design the experiments, guided the ideas, provided important review of the manuscript.

Chapter 4: Rajoana Rojony wrote the discussion and conclusions.

TABLE OF CONTENTS

Page

TABLE OF CONTENTS (continued)

Page

TABLE OF CONTENTS (continued)

Page

TABLE OF CONTENTS (continued)

Page

LIST OF FIGURES

Chapter 1: Introduction

Nontuberculous Mycobacteria (NTM)

The genus Mycobacteria is Gram-positive, aerobic, non-motile, acid-fast and non-spore-forming rods. Many species within the genus Mycobacterium other than *Mycobacterium tuberculosis* complex and *Mycobacterium leprae* are grouped as Non-Tuberculous mycobacteria (NTM) [1][2]. NTMs includes both fast and slow-growing species, and ranging from non-pathogenic to opportunistic pathogens [3][4]. NTMs are ubiquitous in the environment, which includes natural water, human-engineered drinking water systems, bathrooms and soils [5]. In the environment, NTM can form biofilm, and it is described to be relatively resistant to antibiotics, disinfectant, and heavy metals [6]. More than 160 different species of NTM have been identified [7]. NTMs mainly cause pulmonary disease in immunocompromised patients such as AIDS or in-patient with underlying lung conditions such as cystic fibrosis, bronchiectasis or chronic obstructive lung disease [8]. Seventy seven percent of NTM infection manifest as pulmonary illnesses but the bacteria can also infect skin, bones, joints, central nervous system, wound, the lymphatic system, and soft tissue [9].

The *Mycobacterium avium* complex (MAC) and *Mycobacterium abscessus* are the most common species isolated from the respiratory tract and associated with clinical NTM pulmonary diseases. They account for more than 90% of the all cases reported worldwide [8]. MAC consists of two mycobacterial species: *M. avium* subspecies and *Mycobacterium intracellulare. M. avium* consists of four distinct subspecies (*Mycobacterium avium subspecies hominissuis (*MAH), *M. avium subsp. paratuberculosis, M. avium subsp. avium, and M. avium subsp. silvaticum)* [10]. *M. abscessus* complex another clinically important NTM is currently divided into 3 subspecies: *M. abscessus* subspecies *abscessus* (MAB); *M. abscessus* subspecies *massiliense* and *M. abscessus* subspecies *bolletii* [13]. *M. abscessus* group is rapid-growing, non-pigmented, acid-fast and slightly Gram-positive bacilli, that are responsible for a wide range of diseases. *Mycobacterium abscessus* mainly causes pulmonary infections, also responsible for traumatic contaminated skin injury

infection, nonsterile post-surgical soft tissue infection, central nervous system infections, bacteremia, and other infections [13].

Epidemiology of Nontuberculous Mycobacteria:

Infections caused by *Mycobacterial tuberculosis* complex are the most common cause of mortality and morbidity in developing countries of South-East Asia, Western Pacific regions and in African regions [14][15]. Because of *Mycobacterial tuberculosis* clinical significance, it is one of the most studied bacterial pathogens in the world, although nontuberculous mycobacterial infection is an increasing problem in industrialized countries. NTMs disease is not reportable to public health authorities; therefore, little is known about the prevalence and the profile of NTMs.

With the improvement in methodology in the mycobacteriology laboratory, a dramatic increase in prevalence and isolation has been observed in North America from 1980 in older population, patient with an underlying lung condition, immunocompromised due to HIV infection [16]. North American study report demonstrated that from pulmonary NTM infection MAC was the common (80.1%) isolated organism, followed by *M. abscessus* (12.1%), *M. fortuitum* (5.6%), and *M. kansasii* (5.5%) [17]. As NTMs are commonly isolated from water, the prevalence of NTM pulmonary disease in the United States are more associated with ocean coastlines and higher in Sothern than northern states [18].

A systemic review article depicted NTM epidemiology in Asia and among cases, MAC was the most commonly isolated followed by rapidly growing mycobacteria (*M. chelonae, M. fortuitum, M. abscessus*) [19].

The increase in HIV prevalence in developed countries had a huge contribution to a rise in NTM infections. One study of Memorial Sloan-Kettering Cancer Center in New York found that 30 out of 50 AIDS patients had disseminated MAC infection between 1981 to 1984 [20].The antiretroviral therapy in 1996 reduced MAC in AIDS patients, but there was a rise in infections between 1995–1999 in non-HIV patients with a peak rise in infections in 1997 [21].

The laboratory survey by the Centers for Disease Control and Prevention from 1993 to 1996 showed the rate of positive NTM cultures was 7.5–8.2 cases per 100,000 persons. A study conducted in one large hospital in New York from 2000-2003 found positive culture rate of 17.7 per 100,000 persons [22]. Another study in Oregon, USA, reported NTM prevalence to be 8.6 per 100,000 in the 2005-2006, after age adjustment the prevalence has increased by 20.4 per 100,000 in those individuals over 50 years old [23]. Over the 11 year period, from 1999-2010 NTM disease mortality in the United States rose from 0.069 to 0.077 per 100,000 person-years [24].

Treatment of NTM

Treatment of NTM varies with bacterial species. The main challenge of treating NTM infected patients is the use of several compounds, as combination therapy, for a prolonged period of time. Combination therapy for MAC infection, in general, relies on a macrolide-based (clarithromycin or azithromycin) therapy and includes ethambutol and a rifamycin (rifampin or rifabutin) [25]. MAC disease associated with a cavitary lesion and in advanced cases of MAC infection, aminoglycosides (amikacin or streptomycin) are added based on patients tolerability [26]. Some recent studies suggested that amikacin liposomal formulation called Amikacin liposome inhalation suspension (ALIS) intranasal instillation administration is an effective therapy for NTM including MAC. The administration by intranasal route minimize systemic toxicity. ALIS has been approved for the treatment of MAC lung disease in the USA [27].

Therapy of *M. abscessus* (MAB) is very challenging, as it is the most resistance pathogenic NTM. There are no recommended current guidelines for *M. abscessus* infection treatment. Treatment of MAB is individual specific, in general relies on a sensitivity test from macrolide (clarithromycin or azithromycin) group of drugs. MAB infected patients treated with macrolide drug combined with intravenous amikacin with cefoxitin or imipenem [28]. Cefoxitin, imipenem, and amikacin are typically used to treat *M. abscessus* pulmonary infection, as macrolides are generally ineffective against two subspecies of *M. abscessus* because of erm gene (41), an inducible macrolide

resistance gene [29]. Recently a new *Drosophila melanogaster–M. abscessus* infection model showed that tigecycline, linezolid and clarithromycin were the best combination to increase the lifespan of M. abscessus-infected Drosophila [30].

NTM Biofilms

Biofilms are bacterial cells aggregates at a surface, where bacteria are encapsulated in an extracellular matrix of their own synthesis [31]. In most bacterial biofilms, the extracellular material called matrix accounts for over 90% of dry mass and microorganisms account for less than 10%. The biofilm matrix composed of mainly exopolysaccharide, proteins, DNA, lipids and other molecules [32]. The NTM extracellular polymeric matrix material varies within interspecies. The composition of biofilm matrix of different NTMs is not well characterized [33]. The NTMs lipid part of biofilms matrix are related to the specific bacterial cell envelop. MAC, *M. abscessus*, and *M. smegmatis* cell wall glycopeptidolipids are found in their biofilm matrix [34][35].

The NTMs are found ubiquitously in natural waters, engineered water systems, and soils. Biofilm formation by NTM leads to increase bacterial survival, persistence, and growth in environment [3]. As biofilm formation is a successful bacterial survival strategy, bacteria in biofilm shown to be 10- to 1000-folds higher drug resistant than their planktonic counterpart. Formation of biofilms by NTM in human and animals increases bacterial survival, and gives them an inherent resistance to antimicrobial agents, makes bacterial infection persistent and chronic. For this reason, NTM biofilms formation mechanism, bacterial phenotypic changes within biofilm, biofilm composition and resistance mechanism of NTM against antimicrobials are an important research topic.

The phenotypic remodeling of NTM during biofilm formation induces bacteria to tolerate high concentration of antimicrobials. Lack of adequate nutrient and oxygen within biofilm change bacteria into non-replicating “persisters” Phenotype [32]. On the

other hand, biofilm prevent the optimal penetration of antimicrobials and low metabolism within biofilm interfere with drug killing mechanisms [33].

Scope of the master's thesis:

The driving questions investigated for this master's thesis were: 1) how do *M. avium* subsp. *hominissuis* (MAH) and *M. abscessus* subspecies *abscessus* (MAB), two clinically important NTM alter their metabolism in biofilm and anaerobic conditions? and 2) what are the possible metabolic pathways associated with bacterial tolerance and survival during exposure with antibiotics?

The following two chapters of this thesis aim to answer these questions by identifying global proteomic remodeling of MAH and MAB within the specific niche of different environmental conditions of the host with and without antibiotic treatments. This study establishes global proteomic changes in suppression and synthesis of many enzymes promoting shift in bacterial metabolic state that enhances MAH and MAB tolerance within different environments with or without antimicrobials.

References:

[1] N. Rastogi, E. Legrand, and C. Sola, “The mycobacteria : an introduction to nomenclature and pathogenesis,” Rev Sci Tech. 2001 Apr;20(1):21-54.

[2] V. M. Katoch, “Infections due to non-tuberculous mycobacteria (NTM),” Indian J Med Res. 2004 Oct;120(4):290-304.

[3] J. O. Falkinham, “Surrounded by mycobacteria : nontuberculous mycobacteria in the human environment,” vol. 107, pp. 356–367, 2009.

[4] E. Tortoli, “Impact of Genotypic Studies on Mycobacterial Taxonomy : the New Mycobacteria of the 1990s,” vol. 16, no. 2, pp. 319–354, 2003.

[5] J. O. F. Iii, “Nontuberculous mycobacteria in the environment,” vol. 23, p. 24061, 2002.

[6] J. O. Falkinham and V. Tech, *“The Impact of Human Activities on the Ecology of Nontuberculous Mycobacteria.”* Future Microbiol. 2010 Jun;5(6):951-60. doi: 10.2217/fmb.10.53.

[7] J. E. Stout, W. Koh, and W. Wai, “International Journal of Infectious Diseases Update on pulmonary disease due to non-tuberculous mycobacteria,” *Int. J. Infect. Dis.*, vol. 45, pp. 123–134, 2016.

[8] M. Wu, D. B. Aziz, V. Dartois, and T. Dick, “NTM drug discovery : status , gaps and the way forward,” Drug Discov Today. 2018 Aug;23(8):1502-1519. doi: 10.1016/j.drudis.2018.04.001. Epub 2018 Apr 7.

[9] P. M. Cassidy, K. Hedberg, A. Saulson, E. Mcnelly, and K. L. Winthrop, “Nontuberculous Mycobacterial Disease Prevalence and Risk Factors : A Changing Epidemiology,” Clin Infect Dis. 2009 Dec 15;49(12):e124-9. doi: 10.1086/648443.

[10] C. B. Inderlied, C. A. Kemper, and L. E. M. Bermudez, “The Mycobacterium avium Complex,” Clin Microbiol Rev. 1993 Jul;6(3):266-310

[11] S. K. Field and D. Fisher, “pulmonary disease in patients without HIV infection,” Chest 2004;126;566-581.

[12] J. O. F. Iii, “Epidemiology of Infection by Nontuberculous Mycobacteria,” vol. 9, no. 2, Clin Microbiol Rev. 1996 Apr;9(2):177-215.

[13] B. Petrini, “Mycobacterium abscessus : an emerging rapid-growing potential pathogen,” APMIS. 2006 May;114(5):319-28.

[14] “World Health Organization global TUBERCULOSIS Executive summary report 2018,” 2018.

[15] S. K. Brode, C. L. Daley, and T. K. Marras, “The epidemiologic relationship between tuberculosis and non- tuberculous mycobacterial disease : a systematic review,” vol. 18, no. February, pp. 1370–1377, 2014.

[16] K. L. Winthrop, “Pulmonary disease due to nontuberculous mycobacteria: an epidemiologist’s view “,Future Microbiol. 2010 Mar;5(3):343-5. doi: 10.2217/fmb.10.13

[17] U. States *et al.,* “Nontuberculous Mycobacteria – associated Lung Disease in Hospitalized Persons ,” vol. 15, no. 10, pp. 1998–2005, 2009.

[18] S. E. Strollo, J. Adjemian, M. K. Adjemian, and D. R. Prevots, “The Burden of Pulmonary Nontuberculous Mycobacterial Disease in the United States,” vol. 12, no. 10, 2015.

[19] S. Simons *et al.*, “Nontuberculous Mycobacteria in Respiratory Tract Infections , Eastern Asia,” vol. 17, no. 3, 2011.

[20] T. E. Kiehn *et al.*, “Infections Caused by Mycobacterium avium Complex in Immunocompromised Patients : Diagnosis by Blood Culture and Fecal Examination , Antimicrobial Susceptibility Tests , and Morphological and Seroagglutination Characteristics,” vol. 21, no. 2, pp. 168–173, 1985.

[21] M. T. Henry, L. Inamdar, D. O. Riordain, M. Schweiger, and J. P. Watson, “Nontuberculous mycobacteria in non-HIV patients : epidemiology , treatment and response,” Eur Respir J. 2004 May;23(5):741-6.

[22] E. E. Bodle, J. A. Cunningham, P. Della-latta, N. W. Schluger, and L. Saiman, “Epidemiology of Nontuberculous Mycobacteria in Patients without HIV Infection , New York City,” vol. 14, no. 3, 2008.

[23] K. L. Winthrop *et al.*, “Pulmonary Nontuberculous Mycobacterial Disease Prevalence and Clinical Features An Emerging Public Health Disease,” vol. 2006, no. 4, pp. 2005–2006, 2006.

[24] M. Mirsaeidi, R. F. Machado, J. G. N. Garcia, and D. E. Schraufnagel, “Nontuberculous Mycobacterial Disease Mortality in the United States , 1999 – 2010 : A Population-Based Comparative Study,” vol. 9, no. 3, pp. 1–10, 2014.

[25] D. E. Griffith *et al.*, “American Thoracic Society Documents An Official ATS / IDSA Statement : Diagnosis , Treatment , and Prevention of Nontuberculous Mycobacterial Diseases,” american journal of respiratory and critical care medicine vol 175 2007.

[26] S. H. Kasperbauer and C. L. Daley, “Diagnosis and Treatment of Infections due to Mycobacterium avium Complex,” *Semin Respir Crit Care Med*, vol. 29, no. 5, pp. 569–576, 2008.

[27] M. Shirley, “Amikacin Liposome Inhalation Suspension : A Review in Mycobacterium avium Complex Lung Disease,” *Drugs*, vol. 79, no. 5, pp. 555–562, 2019.

[28] W. Koh *et al.*, “Mycobacterial Characteristics and Treatment Outcomes in Mycobacterium abscessus Lung Disease,” vol. 64, no. 41, pp. 309–316, 2017.

[29] F. P. Maurer, C. Castelberg, C. Quiblier, and E. C. Bo, “Erm (41) -dependent inducible resistance to azithromycin and clarithromycin in clinical isolates of Mycobacterium abscessus,” Journal of Antimicrobial Chemotherapy, Volume 69, Issue 6, June 2014, Pages 1559–1563.

[30] C. Oh, C. Moon, O. K. Park, S. Kwon, and J. Jang, “Novel drug combination for Mycobacterium abscessus disease therapy identified in a Drosophila infection model,” Journal of Antimicrobial Chemotherapy, Volume 69, Issue 6, June 2014, Pages 1599–1607.

[31] J. W. Costerton, P. S. Stewart, and E. P. Greenberg, “Bacterial Biofilms : A Common Cause of Persistent Infections,” vol. 284, no. May, pp. 1318–1323, 1999.

[32] S. Sousa, M. Bandeira, P. Almeida, and A. Duarte, “Nontuberculous mycobacteria pathogenesis and biofilm assembly,” *Int. J. Mycobacteriology*, vol. 4, no. 1, pp. 36–43, 2015.

[33] M. Mcnabe, R. Tennant, L. Danelishvili, L. Young, and L. E. Bermudez, “Mycobacterium avium ssp. hominissuis biofilm is composed of distinct phenotypes and influenced by the presence of antimicrobials,” *Clin. Microbiol. Infect.*, vol. 17, no. 5, pp. 697–703, 2011.

Chapter 2

Quantitative analysis of *Mycobacterium avium subsp. hominissuis* proteome in response to antibiotics and during exposure to different environmental conditions

Rajoana Rojony[1], Matthew Martin[2], Anaamika Campeau[4], Jacob M. Wozniak[4], David J. Gonzalez[4], Pankaj Jaiswal[2], L. Danelishvili[1,*] and Luiz E. Bermudez[1,3,*]

[1]Department of Biomedical Sciences, Carlson College of Veterinary Medicine, Oregon State University

[2] Department of Botany and Plant Pathology, College of Agricultural Sciences, Oregon State University

[3] Department of Microbiology, College of Sciences, Oregon State University

[4]Department of Pharmacology, School of Medicine, Skaggs School of Pharmacy and Pharmaceutical Sciences, University of California San Diego

Submitted to Clinical Proteomics

Abstract

M. avium subsp. *hominissuis* (MAH) belongs to the clinically important non-tuberculous mycobacterial group that infects immunocompromised patients and individuals with underling lung conditions. The need for prolonged therapy is a major challenge of MAH treatment, influencing the development of persistent and drug-resistant infections. The reason why bactericidal drugs take several months to eliminate MAH is unknown. To investigate MAH proteome remodeling under aerobic, anaerobic and biofilm conditions (as it is encountered in patient lungs) and identify metabolic changes potentially associated with bacterial persistent state, we performed the relative protein quantitative analysis using Tandem Mass Tag Mass Spectrometry sequencing. MAH was exposed to amikacin (4μg/ml) and clarithromycin (16μg/ml) under aerobic, anaerobic or biofilm condition for 24h and the response was compared with bacterial proteome expressed under corresponding condition. Overall, 4,000 proteins were identified out of 5,313 MAH genome across all experimental groups. Numerous sets of *de novo* synthesized proteins belonging to metabolic pathways not evidenced in aerobic condition were found commonly expressed in both anaerobic and biofilm conditions, including pantothenate and CoA biosynthesis, glycerolipid metabolism, nitrogen metabolism and chloroalkene degradation, known to be associated with bacterial tolerance in *M. tuberculosis*. The common pathways observed in anaerobic and biofilm conditions following drug treatments were peptidoglycan biosynthesis, glycerophospholipid metabolism and protein export. The LprB lipoprotein, highly expressed in MAH biofilms during drug treatments and shown to be essential for *M. tuberculosis* virulence and survival *in vivo*, was selected and overexpressed in MAH. Results demonstrate that LprB is secreted in MAH biofilms and the overexpression clone is more tolerant to antimicrobials than the wild-type strain. Our study identified promising metabolic pathways that can be targeted to prevent the bacterial tolerance mechanism and, subsequently, reduce the length of MAH therapy.

Introduction

Mycobacterium avium subsp. *hominissuis* (MAH), ubiquitously found in the environment, is an opportunistic pathogen associated with infections in human and other mammals [1]. Individuals with an underlying respiratory disease such as chronic obstructive pulmonary disease as well as cystic fibrosis are predisposed to MAH infection. MAH can also infect patients with immunosuppressed conditions and apparently healthy persons [2]. It is clear that the number of patients with nontuberculous mycobacterial (NTM) lung infections are in the rise in recent years [3].

The treatment of MAH infection, in general, relies on a macrolide-based (clarithromycin or azithromycin) therapy and includes ethambutol and rifampin or rifabutin [4, 5]; however, aminoglycosides (amikacin) are prescribed in advanced cases of infection and in MAH disease associated with a cavitary lesion [5]. Unfortunately, treatment of MAH cavitary lesions with a macrolide and an aminoglycoside results many times in unsatisfactory outcome [3, 6]. The main challenge of treating MAH patients is the inability to rapidly eliminate the infection; even when bactericidal concentrations of compounds are employed, resulting in use of the prolonged treatment. Although, the required extended period of therapy and multidrug treatment result in more favorable outcome for many patients, usually it eradicates MAH infection in only 40% to 60% of individuals [3, 7]. The explanation for an incomplete response to therapy is that the bacterium enters a nonreplicating persistent state and becoming tolerant to antibiotics. A low metabolic state during stress conditions is a common response observed in MAH. Evidence suggests that starvation or limitation in nutrients, low pH and lack of the oxygen induce a nonreplicating state *in vitro* characterized by modification of metabolic state of the pathogen [8]. MAH can survive the rapid shifts in and out of low oxygen condition for prolonged periods of time, by altering their metabolism from aerobic to anaerobic [9]. In addition, the phenotypic remodeling of MAH during biofilm formation facilitates development of bacterial tolerance to antibiotics. Biofilm structure, on the other hand, prevents the optimal penetration of antibiotics and interferes with drug killing mechanisms [10, 11].

Novel treatment approaches are urgently needed against MAH. There is a gap, however, in knowledge on MAH pathogenicity strategies and phenotypic changes associated with bacterial tolerance and survival following exposure with antibiotics. In addition, MAH is exposed to different environments encountered by the pathogen in the lung tissue and intracellularly, such as biofilm and anaerobic conditions.

To gain insights into MAH proteome remodeling under aerobic, anaerobic and biofilm conditions, and determine the pathogen response in each condition following exposure to bactericidal concentrations of effective antimicrobials, we carried out assays that demonstrated bacterial global changes such as the suppression and synthesis of many enzymes, promoting shift of metabolic state and enhancing MAH persistence within different environments. This study also identifies several novel targets that potentially may contribute to rapid killing of MAH.

Materials and Methods

Mycobacteria strains and culture conditions. *Mycobacterium avium* subsp. *hominissuis* 104 (MAH 104) is a virulent strain isolated from the blood of an AIDS patient and can cause pulmonary infections in mice [12]. MAH 104 was cultured onto 7H10 Middlebrook agar or in 7H9 Middlebrook broth (Difco Laboratories, Detroit, MI) supplemented with 10% oleic acid, albumin, dextrose, and catalase (OADC, Hardy Diagnostics, Santa Maria, CA). MAH was incubated at 37°C until mid-log phase of growth (around 7 days). To prepare the inoculum, the bacterial suspension was adjusted to McFarland standard 0.5 (approximately 1.5 x 10^8), and exact inoculum was confirmed by colony forming units (CFUs) where bacterial serial dilutions were plated on 7H10 agar.

Antimicrobial reagents and susceptibility testing. Amikacin (AMK) was purchased from the Sigma-Aldrich and clarithromycin (CLA) from TCI AMERICA. Amikacin and clarithromycin were solubilized in water and acetone, respectively. Susceptibility to drug concentrations in the range of 0.065 – 128 μg/ml were performed by the microdilution method in Hank's Balanced Salt Solution (HBSS). Briefly, 3×10^5 bacteria/ml were cultured in 7H9 Middlebrook broth supplemented with or without compounds and grown in a shaker at 37°C for 7 days. Minimal Inhibitory Concentrations (MICs) were visually determined at day 7. Bactericidal concentrations were established by centrifuging tubes at 3,500 rpm for 30min and plating serially diluted bacterial pellets on 7H10 agar. Plates were incubated at 37°C for 10 days. The drug concentration that inhibit 99.9% bacterial growth was considered as the bactericidal concentration.

MAH killing kinetics *in vitro*. Approximately $3x10^5$ bacteria were inoculated into 3ml of 7H9 broth containing either AMK 4μg/ml, 16 μg/ml CLA or no antibiotic. Samples were incubated under 200 rpm agitation at 37°C and, after 24 h, 48 h, 72h and 96h exposure, centrifuged for 30 min at 3,500 rpm, serially diluted and plated onto 7H10

agar plates for CFU determination. To establish the MAH killing dynamics under an anaerobic condition, a suspension of $3x10^5$ bacteria were inoculated into 3ml of 7H9 broth, with and without antibiotics, and tubes were placed into anaerobic jars (BD BBL™ GasPak™ Jar). The anaerobic BD BBL™ GasPak™ and CO_2 indicators were inserted inside the jar and the grease was applied over the rim to seal the Jar tightly. The anaerobic jars (one jar for each time point) were kept in the shaker incubator at 37°C with gentle agitation (30 rpm). At selected time points, the jar was opened, tubes were removed and centrifuged at 3,500 rpm for 30 min. Pellet was resuspended in PBS, serially diluted and plated into 7H10-agar plate to CFU/ml counts. In addition, the killing kinetic was determined under the biofilm condition as well. Two hundred microliter of $3x10^6$ bacterial inoculum prepared in HBSS was distributed into 96-well tissue culture plates, covered with a cellophane membrane and kept at 25°C for 7 days. After 7 days, the entire supernatant was removed and replenished with fresh HBSS containing bactericidal concentration of antibiotics, or lack of antibiotics. At selected time points, the biofilms were disrupted to obtain even suspensions and plated for viable bacteria counts. The experiment was carried out in duplicate and repeated three independent times.

MAH killing kinetics in human macrophages. Human THP-1 cell line (TIB-202) was purchased from the American Type Culture Collection (Manassas, VA). Cells were cultured in RPMI-1640 medium supplemented with heat-inactivated 10% fetal bovine serum (FBS, Gemini Bio-products, Sacramento, CA), L-glutamine, and 25 mM HEPES (Corning, Manassas, VA) at 37°C with 5% CO_2 and maintained in $75cm^2$ tissue culture flasks. THP-1 monocytes were differentiated into macrophages using 10 ng/ml of phorbol 12-myristate 13-acetate (PMA, Sigma-Aldrich). Intracellular antibiotic killing assays were performed as previously described with minor modifications [13]. Briefly, PMA treated THP-1 cells were seeded into 48-well plates at 90 to 100% confluence (3×10^5/well), matured and 24h latter monolayers were replenished with fresh medium. Monolayers were allowed to rest for an additional 48h, and then infected with MAH 104 for 2h at a multiplicity of infection (MOI) of 10. Extracellular bacteria were

subsequently removed by both washing three times with HBSS and treating monolayers with 400 μg/ml amikacin for 1h. Infected monolayers were treated with either AMK 4μg/ml, 16 μg/ml CLA or no antibiotic as a control. THP-1 cells were replenished with new media containing antibiotics, or no antibiotic, every other day. Cells were lysed at 2h (baseline), day 1, day 3 day 5 and day 7 followed by plating on 7H10 agar plates to determine the number of viable intracellular bacteria. For macrophage infection and antibiotic killing assay with MAH104 pre-incubated under anaerobic condition, bacterial suspension in HBSS was kept in the anaerobic chamber for 24h at 25°C, and then used as an inoculum to infect THP-1 cells with MOI of 10. To express the biofilm phenotype, we formed MAH biofilms for 7 days and then dispersed for the inoculum preparation as described above. Cells were replenished with fresh media containing antibiotics or no antibiotic every other day and lysed at 2h (baseline), day 1, day 3 day 5 and day 7 to determine the number of viable intracellular bacteria.

Sample preparation for proteomic sequencing. Approximately, $1x10^8$ *M. avium* 104 cells/ml of were inoculated in 10ml of 7H9 culture media in the $25cm^2$ tissue culture flasks supplemented with bactericidal concentrations of AMK or CLA for 24 h. For the aerobic condition, tubes were kept in the shaker at 37°C and for the anaerobic condition samples were placed into anaerobic jar at 37°C. In addition, biofilms were formed for 7 days in 10 ml HBSS using $1x10^8$ cells/ml inoculum in the $25cm^2$ tissue culture flasks. After, the supernatant was gently removed and replenished with the fresh HBSS containing antibiotics for additional 24 h. Next, samples were centrifuged at 3,500 rpm for 20 min at 4°C, pellets were washed once with HBSS and resuspended in 3% SDS containing EDTA-free Protease Inhibitor Cocktail (Sigma-Aldrich). Bacterial cells were mechanically disrupted through bead-beating, cleared through microcentrifugation at 15,000 rpm for 10 min and filtration using the 0.22μm syringe filters. Total protein concentrations were measured using Thermo Scientific NanoDrop machine.

Tandem Mass Tag (TMT) labeling and Liquid chromatography–mass spectrometry (LC-MS). Precleared lysates were immersed in equal volumes of 8 M urea and a lysis buffer containing 75 mM NaCl, 3% sodium dodecyl sulfate (SDS), 1 mM sodium fluoride, 1 mM beta-glycerophosphate, 1 mM sodium orthovanadate, 10 mM sodium pyrophosphate, 1 mM phenylmethylsulfonyl fluoride, 1X complete EDTA-free protease inhibitor cocktail (Roche), and 50 mM HEPES (Sigma), pH 8.5. Samples were subjected to pulsed probe sonication to ensure complete cell lysis. A pulse protocol of 15 seconds "on" at 20% amplitude was alternated with 15 second periods of rest three times. Disulfide bonds were reduced in 5 mM of dithiothreitol (DTT) for 30 minutes at 56°C. Reduced cysteine residues were alkylated in 15 mM of iodoacetamide (IAA) for 20 minutes in a darkened environment at room temperature. The alkylation reaction was subsequently quenched by the addition of the original added volume of DTT and incubation of the solution in a darkened environment at room temperature for 15 minutes [14].

Protein was precipitated by adding one quarter of the total sample volume of trichloroacetic acid (TCA) to the sample solution. Samples were vortexed and incubated on ice for 10 minutes before being subjected to centrifugation at 14,000 rpm for an additional 2 minutes. The resultant supernatant was removed and samples kept on ice for the subsequent wash steps. Samples were washed in 300 µL of ice-cold acetone and subjected to centrifugation at 14,000 rpm for 2 minutes. The supernatant was removed and the acetone wash step repeated. After removal of the second acetone wash supernatant, samples were dried on a 56°C heating block. Samples were resuspended in 300 µL of a solution of 1 M urea and 50 mM HEPES, pH 8.5. Resuspended samples were subjected to 5 minutes of vortex-agitated and 5 minutes of water bath sonication. Samples were then subjected to a two-step digestion [15]. First, 3 µg of sequencing-grade LysC was added and samples were incubated on a shaker at room temperature overnight. Second, 2.8 µg of sequencing-grade trypsin was added to the samples and were incubated at 37°C for 6 hours. Samples were acidified by the addition of 20 µL of 10% trifluoroacetic acid and were desalted on C18 columns using previously-described methods [16]. Samples were lyophilized at this stage.

Lyophilized samples were immersed in a solution of 50% acetonitrile and 5% formic acid prior to quantification. Peptide quantification was performed using the Pierce Quantitative Colorimetric Peptide Assay (Thermo). Fifty µg of each sample was separated for tandem mass tag (TMT) labeling [17, 18]. An internal standard containing an equal mass of each sample was prepared, and 50 µg of the standard was separated per intended set of 10 TMT labels. Sample aliquots designated for further analysis were lyophilized.

Lyophilized samples were resuspended in 50 µL of a solution of 30% anhydrous acetonitrile and 200 mM of HEPES, pH=8.5. TMT labels were resuspended in 40 µL of anhydrous acetonitrile and subjected to vigorous shaking for 5 minutes. A TMT label assignment scheme was generated using two core principles: first, no two experimental replicates were assigned to the same label, and second, each experimental condition was represented in each set of 10 labels. Eight µL of each label was added to the designated sample, and the labeling reaction was allowed to proceed at room temperature for 1 hour. Reaction quenching was performed by the addition of 9 µL of a solution of 5% hydroxylamine and room temperature incubation for 15 minutes. Reactions were acidified through the addition of 50 µL of a solution of 1% TFA. Samples assigned within each set of 10 labels were mixed, and each resulting mixture was desalted on C18 columns using the same methods as above.

Multiplexed samples were subjected to basic reverse phase liquid chromatography on an Ultimate 3000 HPLC with 4.6 mm x 250 mm C18 resin column. Samples were resuspended in 120 µL of a solution of 5% acetonitrile and 5% formic acid and loaded onto the column. Samples were eluted as 96 fractions on a gradient ranging from 5% to 35% acetonitrile in 10 mM ammonium bicarbonate. Fractions were concatenated as described previously, and alternating concatenated fractions were lyophilized [19]. Lyophilized fractions were resuspended in a solution of 5% acetonitrile and 5% formic acid prior to analysis by LC-MS.

All mass spectrometry-based analysis was performed on an Orbitrap Fusion Tribrid Mass Spectrometer with in-line Easy nLC System at the University of California San Diego

Mass Spectrometry Facility. Samples were loaded onto a column pulled and packed in-house. The inner diameter of the column was 100 µm and the outer diameter was 350 µm. The contents of the column were as follows: the distal tip was packed with 0.5 cm of 5 µm C4 resin followed by 0.5 cm of 3 µm C18 resin. The remaining 29 cm was packed with 1.8 µm C18 packing resin. Peptides were eluted on a 165-minute gradient ranging from 11% to 30% acetonitrile in 0.125% formic acid at a flow rate of 300 nL/min. The column was heated to 60°C.

All data were acquired in centroid mode. Electrospray ionization was achieved through the application of 2000 V of electricity through a T junction connecting sample, waste and column capillaries. MS1 spectra were collected in data-dependent mode using a scan range between 500-1200 m/z with resolution of 60,000. Automatic gain control was set to $2x10^5$ and the maximum inject time was 100 ms. The top N method for peak selection was selected, with N set to 10 for MS2 and MS3 analysis. Parent ions were selected in the quadrupole at 0.5 Th for MS2 fragmentation. Parent ions were fragmented using collision-induced dissociation (CID) energy and fragment ions were detected in the ion trap with a rapid scan rate automatic gain control of $1x10^4$. TMT reporter ion fragmentation was performed using synchronous precursor selection (SPS). The MS2 precursors chosen were fragmented using high-energy collisional dissociation (HCD). Reporter ions were detected in the Orbitrap. The lower limit of detection at the MS3 stage was set to 110 m/z and automatic gain control was set to $1x10^5$. The maximum inject time was 100 ms.

MS data processing. Raw data files were searched using Proteome Discoverer 2.1 using SEQUEST-HT[20]. The reverse database strategy for decoy database generation was used [21-23]. Files were searched against the MAH 104 strain reference proteome. The precursor and fragment ion mass tolerances were set to 50 ppm and 0.6 Da, respectively. The digesting enzyme was specified as trypsin, and up to two missed cleavages were allowed. Peptides of fewer than 6 amino acids or more than 144 amino acids were excluded. A dynamic modification of methionine oxidation (+15.995 Da) was included in the search parameters, as were static modifications for isobaric tandem

mass tags at the N-termini and on lysine residues (+229.163 Da) and carbamidomethylation of cysteine residues (+57.021 Da). Filtering of spectra was performed in Percolator at the peptide and protein levels at a 1% FDR threshold.

Resultant peptide spectral matches were manually filtered to exclude spectra without high confidence, with rejected PSM ambiguity status, with isolation interference larger than 25 and with average signal to noise value of less than 10. TMT relative abundance values were summed within proteins matches. Data normalization was performed using a two-step process. TMT signal to noise values were first normalized to the pooled internal standard divided by the median of all internal standard values. The resultant values were then normalized to median signal to noise values for each label divided by the median of all channel median values to account for variable labeling efficiencies.

The identified MAH proteins were classified into several distinct groups, based on their molecular function. The functional classification was conducted by blasting the amino acid sequence of MAH proteins against the protein sequence database of *M. tuberculosis* strain H37Rv, using the Institute Pasteur's TubercuList web server (http://genolist.pasteur.fr/TubercuList/). MAH unmatched proteins were classified based on their predicted function or grouped into the hypothetical class.

Construction of MAH overexpression clones. The MAV_1423 gene, encoding the lipoprotein LprB, was amplified from the MAH genomic DNA (Forward 5′ TTTTTGGATCCACATCATCATCATCATCATACGATCCTGA 3′ and Reverse 5′ TTTTTGAATTCTCATTTCGAGTTCGC 3′) and cloned either into the BamH1 and EcoRI restriction sites of the pMV261 mycobacterial shuttle plasmid. The His-tag was incorporated into the forward primer. In addition, the LprB gene was also cloned into HindIII and HpaI restriction sites of the pMV261:RFP:His vector containing the Red Fluorescent Protein and His-tag using the forward 5′ TTTTTAAAGCTTCGATCCTGATCCCC 3′ and reverse 5′ TTTTTGTTAACTCATTTCGAGTTCGCAAT 3′ primers. The resulted pMV261:LprB and pMV261:RFP:LprB vectors were transformed into MAH

competent cells that were prepared by washing bacterial pellet four-times with a chilled wash buffer (10 % glycerol and 0.1 % Tween-20). The final pellet was resuspended with 1ml of 10 % glycerol. Two hundred µl of competent MAH Cells were electroporated with 7-µl of plasmid DNA using the Gene Pulser Xcell™ Electroporation Systems and kept for 12h at 37 °C in 7H9 broth. Next, transformed cells were plated on 7H10 agar containing 400 µg/ml of kanamycin. After 14 days of incubation at 37 °C, MAH colonies were screened with PCR for presence kanamycin gene using the following primers: Forward 5′ GTGTTATGAGCCATATTC 3′ and Reverse 5′ TGCCAGTGTTACAACCAA 3′. The PCR program was as follows: 95 °C for 5 min, 35 cycles of 95 °C for 30 s, 57 °C for 30 s, 68 °C for 1 min and a final extension of 68 °C for 5 min. The positive colonies were grown into 7H9 broth supplemented with 400 µg/ml kanamycin.

The LprB overexpression clone susceptibility to antibiotics. *In vitro* antibiotic killing assay was performed as described above. Briefly, $3x10^5$ cells/ml of MAH104 overexpressing the LprB protein were exposed to 4µg/ml AMK or 16 µg/ml CLA for 24 h, 48 h, 72 h and 96 h, serially diluted and plated on 7H10 agar plates for CFU counts. The LprB clone growth without antibiotic treatment and MAH 104 clone containing an empty plasmid with and without antibiotic treatment served as controls.

Biofilm assay. The MAH biofilm formation was examined using the crystal violet staining method as previously described [10]. Approximately, $3x10^8$ cells of the pMV261:RFP:LprB overexpression clone and the wild type MAH 104 were resuspended in per ml of HBSS and 300 µl was added into each well of 96-well plate. Plates were incubated at 25°C in the dark up to 15 days. In addition, to determine if amikacin had enhanced effect on biofilm formation of LprB overexpression clone, 4µg/ml AMK was added to both the wild type and LprB overexpressing wells. The biofilm formation was quantified at 4, 10 and 15 days by removing supernatant from wells and adding 125µl of a 1% crystal violet solution for 15 min at room temperature.

Next, plates were rinsed four times with HBSS and kept upside down for 30 min. Crystal violet was solubilized in 70µl of 30% acetic acid at room temperature for 15 min and an optical density was measured at A570 in a plate reader (Epoch Microplate Spectrophotometer, BioTek).

Macrophage uptake assay using the LprB overexpression clone. Approximately, $3x10^5$ THP-1 cells were seeded and differentiated in 24-well plates. Confluent monolayers were infected with MAH clone overexpressing the pMV261:LprB construct at MOI of 10 bacteria :1 cell. After 15 min, 30 min, 1 h and 2 h of infection, THP-1 macrophages were washed three times with HBSS, lysed, serially diluted and plated on 7H10 agar to determine CFUs. MAH carrying the empty pMV261 plasmid was used as a control clone for invasion assay, and the uptake percentage was compared between experimental and control groups at each time point.

Fluorescence microscopy. Approximately, 200 µl of $3x10^8$ bacterial cells/ml containing either pMV261:RFP or pMV261:RFP:LprB vector were inoculated in to 8-chamber slides, and biofilms were formed for 7 days at 25°C. At day 7, wells were fixed with 4% paraformaldehyde and bacterial biofilms were examined using the fluorescent microscope.

Biofilm matrix preparation. The RFP control and LprB:RFP clones of MAH were incubated for seven days in HBSS to form biofilms in 75 cm^2 flasks. Biofilms were extracted as previously described [24]. Briefly, using a sterile swab, biofilms were collected and pelleted by centrifugation at 2,500 x *g* for 15 minutes. The biomass pellet was resuspended into 1 ml of HBSS and physically agitated in a Mini-Beadbeater-1 (Biospec Products, Bartlesville, OK) without beads to prevent bacterial lysis. Next, samples were microcentrifuged at 12,000 x *g* for 5 minutes to pellet the bacteria and

retain the solubilized matrix in suspension. The supernatants were filtered through a 0.2µm syringe filter to separate total proteins from the matrix.

Statistical analysis. Statistical significance for binary comparisons was performed on proteomics data using the Student's t-test. The f-test was employed to ensure that the statistical assumption of equal variance required for the Student's t-test was met; if it was not, the Student's t-test with Welch's correction was used. Volcano plots were constructed using GraphPad Prism 7. K means clustering was performed on proteomic datasets using the Morpheus K-means clustering tool (https://software.broadinstitute.org/morpheus/).The appropriate number of clusters was determined using the elbow method.

Experiments were repeated at least three times, and the results are expressed as a mean ± standard deviation. The comparisons among experimental groups were performed with ANOVA and Student's t-test when appropriate. A p value of < 0.05 was considered to be statistically significant.

Results and Discussion

Delayed killing of MAH by antimicrobials. Using the broth microdilution method, we have determined that the minimal inhibitory concentration at which 90% of MAH growth was inhibited by AMK and CLA was 1μg/ml for both compounds; whereas the bactericidal concentrations were 4 μg/ml for amikacin and 16 μg/ml for clarithromycin. The antibiotic killing dynamics were investigated in aerobic, anaerobic and biofilm conditions for 4 days (Figure 2.1A). While significant reduction in bacterial viability was observed in the aerobic condition following AMK and CLA treatment over time, a slight decline in MAH CFU/mL was seen for each treatment in the anaerobic and biofilm conditions when compared to no antibiotic control.

MAH killing dynamics by antimicrobials in human macrophages. THP-1 monolayers were infected with MAH expressing either aerobic, anaerobic or biofilm phenotypes. For each phenotype, bacterial survival rate within macrophages without antimicrobial treatment served as a control. As shown in the Figure 1C, THP-1 cells had increased uptake of MAH of the anaerobic and biofilm phenotypes when compared with invasion rates of aerobic bacteria. Furthermore, MAH grown under aerobic conditions had delayed killing kinetics in macrophages when exposed to antimicrobials and, even after 7 days of exposure to bactericidal concentrations of antimicrobials, host cells were unable to clear the infection (Figure 2.1B) resulting in 2- and 3.5-log decrease of intracellular bacteria during AMK and CLA treatment at day 7, respectively. While MAH of anaerobic condition grew within macrophages similarly as the aerobic bacteria, MAH of biofilm phenotype showed a little growth initially within the THP-1 cells, even without any antibiotic treatment, but regained the growth after 3 days. Upon exposure to antibiotics both AMK and CLA exhibited significantly lower killing effects on MAH of both anaerobic and biofilm phenotypes. As demonstrated in the Figure 2.1C, anaerobic bacteria had its growth maintained intracellularly even in presence of antibiotics and showed only 1- or 1.5-log decrease during AMK and CLA treatment at day 7, respectively. In contrast, the MAH with the

biofilm phenotype showed 2- and 3-log decrease in intracellular number of bacterial during AMK and CLA treatment at day 7, respectively (Figure 2.1B).

Global proteome response of MAH under aerobic, anaerobic and biofilm conditions and upon exposure to antimicrobials. To identify proteomic changes *that* MAH undergo in conditions encountered within lung tissues of infected patients and during treatment with antimicrobials, we investigated MAH response to aerobic, anaerobic and biofilm conditions and to AMK and CLA treatments. The quantitative TMT Mass Spectrometric sequencing was performed for samples collected at 24 h time point and, overall, 4,000 proteins were identified across all experimental and control groups. The identified protein list along with their normalized spectral counts, annotations and fold changes over control at corresponding time points for each condition and antimicrobial is presented in the supplemental material. While volcanic plots presented in the Figure 2.2 gives a global overview of induced and repressed proteins following bacterial exposure to different environmental conditions and antibiotics. More specifically, while the incubation under anaerobic and biofilm conditions resulted in upregulation of 409 and 603 proteins, 522 and 585 proteins were downregulated when compared to MAH of aerobic condition. Proteome analysis of MAH treated with AMK for 24 h revealed 263, 17, 41 expressed and 178, 8, 9 downregulated proteins in aerobic, anaerobic and biofilm conditions, respectively, when compared to control no drug treatment group. In presence of CLA, 379, 28, 380 proteins were upregulated and 598, 50, and 107 proteins were downregulated in aerobic, anaerobic and biofilm conditions, respectively, when compared with only control conditions. Histograms of the Figure 2.3 demonstrate the distribution of the average fold changes for proteins at different environment conditions with or without drug treatments.

For a global overview of proteomic changes in MAH response to conditions and antibiotics, without exclusively focusing on the induced proteins only, we used Morpheus to identify K-means clustering (Figure 2.4A). We compared protein levels in each drug treatment versus untreated bacteria using an analysis paired by antibiotic

and condition. In addition, with the elbow method we found 14 optimal number of clusters. The heat map shows that proteins of 1 and 5 clusters are mainly expressed under biofilm formation when exposed to clarithromycin for 24h. While proteins of 2, 7, 11 and 14 clusters are downregulated in biofilms with and without AMK and CLA treatment, proteins clustered in 4, 7 and 8 groups are highly upregulated in the anaerobic condition with and without AMK and CLA treatment. Pie charts in the Figure 2.4B demonstrate metabolic pathway enrichment related to each cluster.

Functional grouping of 1.5-fold and more synthesized MAH proteins. Mass spectrometric analysis of MAH104 samples found a total of 225 proteins and 304 proteins synthesized 1.5-fold and more during 24h amikacin and clarithromycin exposure in the aerobic condition. We categorized differentially synthesized MAH proteins into functional groups as described in the methods. Most represented categories in the aerobic condition during MAH exposure to both antibiotics were intermediate metabolism and respiration (163 proteins), cell wall and cell processes (95 proteins), regulatory proteins (39 proteins), metabolic enzymes falling into oxidoreductase activity category (34 proteins), information pathway (26 proteins), virulence, detoxification, adaptation (22 proteins), and majority of proteins with unknown function (128 proteins) (Figure 2.5A).

While in the anaerobic condition 344 proteins were upregulated with 1.5-fold and more just in the condition, 24h exposure to AMK and CLA induced 23 and 38 protein synthesis, respectively. The distribution of represented categories was the following: 141, 2 and 2 proteins of the intermediate metabolism and respiration, 26, 2 and 2 of regulatory proteins, 8, 6 and 2 proteins from the virulence, detoxification, adaptation group, and enzymes with the oxidoreductase activity were 22, 0 and 3 protein in the anaerobic-no drug, anaerobic-AMK and anaerobic-CLA groups, respectively (Figure 2.5B).

During biofilm formation, MAH synthesized 603 proteins with 1.5-fold and more. The treatment with AMK and CLA of MAH biofilms resulted in 53 and 380 protein

synthesis, respectively. The distribution of represented categories for biofilm-no drug, biofilm-AMK and biofilm-CLA experimental groups were the following: intermediary metabolism and respiration (214, 6 and 148 proteins), regulatory proteins (81, 6 and 13 proteins), in virulence, detoxification, adaptation (17, 1 and 24 proteins), cell wall and cell processes (65, 12 and 54 proteins), lipid metabolism (8, 2 and 32 proteins), information pathways (21, 6 and 46 proteins), proteins with oxidoreductase activity (28, 3 and 12 proteins), and majority of uncharacterized proteins (166, 13 and 48 proteins) (Figure 2.5C).

In addition, the metabolic pathway enrichment in condition and drug treatment groups are presented in Figure 6. The protein assignment to KEGG metabolic pathways showed several over-represented metabolic categories that are further discussed below.

Characterization of MAH metabolic pathways expressed under environmental conditions. Ten metabolic pathways of anaerobic phenotype and nine pathways for biofilm condition were identified to show significant expression when compared with the aerobic condition alone (Figure 2.6A). Among them six pathways were common between anaerobic and biofilm conditions, including the majority of highly synthesized enzymes of chloroalkane and chloroalkene degradation pathways (Figure 2.7A). The chloroalkane pathway leads to the acetaldehyde production, which reversibly can be converted in to an acetyl-CoA, acetyl-p and pyruvate, and then processed in TCA cycle for ATP synthesis. On the other hand, the chloroalkene degradation produces substrate for the glyoxylate cycle, which is a modified Krebs cycle and occurs in mycobacteria. The glyoxylate cycle has a central role in the metabolism of pathogenic mycobacteria and, therefore, enzymes associated with the glyoxylate shunt has been exploited for the development of additional anti-TB therapy [25-28]. Because the isocitrate lyase (ICL) converts the isocitrate into glyoxylate and malate synthase, which in turn catalyzes the malate from glyoxylate, ICL has been proposed to be a potential target for the latent tuberculosis treatment [26, 27]. In addition, some of the glyoxylate could be diverted into the reductive amination pathway to produce NAD from its reduced form [29]. In fact, reductive amination of the glyoxylate by glycine dehydrogenase has been

demonstrated to be an alternative energy source for *M. tuberculosis* during nonreplicative state and aids the pathogen to tolerate the anaerobic condition [30, 31].

While our study identified nitrate, nitrite transporter and nitrite reductase enzymes of MAH highly upregulated under anaerobic and biofilm conditions (Figure 2.7B), in *M. tuberculosis* research, it has been extensively documented that an increased nitrate use had a high impact on bacterial survival during hypoxia by replacing oxygen as terminal electron acceptor [32, 33].

Furthermore, our data shows that histidine metabolism pathway was upregulated in MAH biofilm when compared with bacteria of the aerobic phenotype (Figure 2.7C). It is known that the histidine metabolism is an important pathway promoting bacterial biofilm formation [34-36]. A proteomic study of *Acinetobacter baumannii* biofilms and functional analysis using the gene knockout mutants reveled several cell surface proteins implicated in biofilm formation were also associated with the histidine metabolism [37]. In *Staphylococcus xylosus* research, it has been demonstrated that histidine metabolism has a role on the *S. xylosus* biofilm formation, also IGPD enzyme (imidazoleglycerol-phosphate dehydratase) involved in histidine metabolism played a crucial role in a fourth-generation cephalosporin (cefquinome) inhibition of biofilm formation [38, 39]. In addition, while both auxotrophic and wild-type strains of *M. tuberculosis* are able to survive prolonged starvation, the histidine auxotroph clone is unable to survive a single-amino-acid starvation [40]. In our study, we found that imidazoleglycerol-phosphate dehydratase (hisB/MAV_3185) as well as other enzymes (hisD/MAV_3187, hisC/MAV_3186, hisI/MAV_3180, hisH/MAV_3184) related to the histidine metabolism were highly expressed under biofilm conditions and raises the possibility that histidine may play an important role during MAH biofilm formation and under oxygen starvation either by be converted into other biological active amines or converted to 4-imidazolone-5-propionate in a sequence of reactions resulting in formation of glutamate and ammonia.

Another pathway upregulated in MAH under the anaerobic and biofilm conditions is glycerophopholipid metabolism. As shown in the (Figure 2.7D), the glycerol and fatty acids are used to form 1, 2-diacyl-sn-glycerol and is processed by MAV_2184 into 1,

2-diacyl-sn-glycerol 3-phosphate during biofilm formation. In contrast, MAV_2816 converts 1, 2 diacyl-sn-glycerol 3-phosphate to triacylglycerol in MAH under anaerobic condition.

Several enzymes of pantothenate and CoA biosynthesis pathways were upregulated in both anaerobic and biofilm conditions (Figure 2.7E). Pantothenate (vitamin B5) is a precursor for the biosynthesis of CoA, a cofactor involved in tricarboxylic acid cycle, phospholipids synthesis, fatty acids synthesis and degradation [41]. The flux of carbon through Acetyl-CoA is difficult during non-replicating condition of MAH. Acetyl-CoA is synthesized from fatty acid degradation and uses the glyoxylate shunt to provide the carbon for carbohydrate synthesis [42]. It has been shown that the panC and panD genes of MAH and *M. tuberculosis* are involved in *de novo* biosynthesis of pantothenate [43]. By infecting immunocompromised SCID mice with *M. tuberculosis* ΔpanCD knockout mutants, it has been observed that animals survived for more than 36 weeks; whereas *M. tuberculosis* WT infected mice survived for only five weeks [44].

The proteome analysis identified the pentose phosphate pathway highly upregulated only in MAH biofilms (Figure 2.7F). In the pentose phosphate pathway, the glucose turnover process leads to the synthesis of NADPH and pentose, essential parts of nucleotides. This pathway also produces the phosphoribosyl pyrophosphate (PRPP) from ribose-5P, which is used in the biosynthesis of histidine and purine/pyrimidine [45]. As highlighted above, the histidine metabolism appears to play a very important role in maintaining of bacterial biofilms.

MAH metabolic pathways expressed under different environmental conditions in presence of antibiotics. We identified seven metabolic pathways expressed under aerobic condition and twelve under biofilm condition when treated with CLA, and the expression of these pathways were significantly greater than the one seen in the aerobic condition alone (Figure 2.6B). The oxidative phosphorylation pathway was more prominent in both aerobic and biofilm conditions during presence of CLA with total of twelve proteins synthesized by several-fold higher than in the control group (Figure

2.8A). While oxygen is the final electron acceptor in aerobic condition, nitrate or fumarate could be used as an electron acceptor in anaerobic conditions [46]. Electron transport in mycobacteria is initiated by NADH dehydrogenases (NDH), succinate dehydrogenases (SDH) and various cytochrome oxidases [47]. Proteins nuoAHKLM (MAV_4033, MAV_4040, MAV_4043, MAV_4044 and MAV_4045) identified in this study belong to the NADH dehydrogenase group; whereas MAV_4300 and sdhA (MAV_4299) are succinate dehydrogenase enzymes and facilitate electron transport in MAH. The succinate dehydrogenase enzymes predominantly act in the citric acid cycle to oxidize succinate to fumarate. Our results demonstrate that, in presence of clarithromycin, the TCA cycle is downregulated and oxidative phosphorylation is upregulated. Increased oxidative phosphorylation in mycobacterial leads to generation of increased transmembrane proton gradient through electron transport chain (ETC) and constitutes the proton motive force (PMF). As a result, protons that translocate through ETC are used by efflux pumps (EPs) to extrude drugs [48]. Thus, in aerobic and biofilm conditions MAH can export clarithromycin. In addition, cytochrome C oxidase and reductases has been shown to regulate this process, and our results identify several proteins related to the cytochrome C oxidase process [48, 49].

Other notably upregulated pathways under anaerobic condition during the presence of clarithromycin are bacterial Sec and Tat secretion systems and quorum sensing related protein MAV_4523 (protein translocase subunit SecE) (Figure 2.8B). The twin-arginine translocation (Tat) system is comprised of three membrane proteins of TatA, TatB and TatC actively involved in transport of unfolded proteins from the cytoplasm to exterior of the cell. TatA (MAV_2409) and TatC (MAV_2410) proteins are also greater synthesized in MAH of aerobic phenotype during exposure to both amikacin and clarithromycin separately over the aerobic control. TatA upregulation is triggered by AMK in MAH during biofilm formation as well. In addition, the mycobacterial translocation channel SecE (MAV_4523) was identified in biofilm and anaerobic tested groups of MAH exposed to AMK for 24h.

As summarized in the Figure 6C, AMK exposure to MAH of aerobic, anaerobic and biofilm phenotypes lead to upregulation of ten, seven and five metabolic pathways,

respectively. The glycerophospholipid, peptidoglycan biosynthesis, bacterial secretion and protein export systems were among common metabolic pathways upregulated in AMK treated experimental group under all three conditions. Penicillin-binding proteins (PBPs) belong to the peptidoglycan biosynthesis pathway and are associated with the final stage of bacterial cell wall assembly (Figure 2.8C). The carboxypeptidase enzyme MAV_4305, a low molecular weight PBP, moderates the degree of cross-linking by removing the terminal D-Ala from the peptidoglycan. The enzyme MAV_4305 can also produce Lys-type peptidoglycan. While MAV_4305 was highly upregulated in biofilms, MAV_3830 (D-alanine--D-alanine ligase) and MAV 2333 (Phospho-N-acetylmuramoyl-pentapeptide-transferase) enzymes had increased expression under aerobic condition during AMK treatment.

The potential changes in structure and hydrophobic properties of the cell wall produce new permeability barrier that can increase tolerance to antibiotics [50, 51]. The mycobacterial cell plasma membrane consists of Phosphatidylethanolamine (PE), phosphatidylserine (PS), phosphatidylinositol (PI), phosphatidylglycerol (PG) and cardiolipin (CL). Deficiency in any of these components of the cell wall effect bacterial susceptibility to antibiotics [52]. MAV_3488, MAV_2184 and MAV_2313 proteins, highly upregulated in AMK treatment group, belong to the enzyme group that is involved in the glycerophospholipid metabolism (Figure 2.8D) and most likely paly role in MAH phenotypic resistance to drugs.

Another prominent metabolic pathway, highly upregulated in aerobic and anaerobic bacteria and triggered by AMK treatment, was the sulfur relay system (Figure 2.8E). A sulfur transfer is required step for synthesis of cofactors of molybdenum and thiamin, and it is carried by unique sulfur carrier proteins MoaD and ThiS activated through adenylation by E1-like enzymes [53, 54]. In this study, cysteine desulfurase (IscS/MAV_3872) was upregulated to donate sulfur for molybodenum cofactor biosynthesis. It has been demonstrated in *Escherichia coli* that IscS converts the MoaD acyl-adenylate into a thiocarboxylate during molybdenum cofactor biosynthesis and supports molybdopterin synthesis [55]. The IscS enzyme has the central role in

donating the sulfur to FeS clusters, the thionucleosides 4-thiouridine and 5-methyl aminomethyl-2-thiouridine and thiamin [56, 57].

Furthermore, proteins of sulfur metabolism, specifically, sulfur assimilation were cysH/MAV_1786 and cysH/MAV_2153 phosphoadenosine phosphosulfate reductase enzymes were upregulated in MAH of aerobic condition during AMK treatment (Figure 8F). The phosphosulfate reductase enzymes convert an adenylyl sulfate (APS) to phosphoadenosine phosphosulfate (PAPS); whereas PAPS is the universal sulfate donor for sulfotransferases. Sulfide is a final product of sulfur metabolism and is used in biosynthesis of coenzymes, S-containing amino acids such as cysteine and methionine, and mycothiol. Thiol containing small detoxifying molecule mycothiol (MSH) removes numerous bactericidal agents to maintain the highly reducing environment within bacteria and protect cells against disulfide stress [48]. We identified the alkanesulfonate monooxygenase (MAV_3426), which is involved in converting alkane sulfonate and methane sulfonate into sulfite and was upregulated in MAH of aerobic phenotype due to AMK treatment. It has been demonstrated that *M. tuberculosis* sulfur metabolism genes, including cysH transcriptional regulator, are highly upregulated in nutrient deprived conditions, hypoxia and sulfite assimilation increases due to exposure to antibiotics [54, 58].

Characterization of LprB lipoprotein. We hypothesized that MAH proteins that are commonly synthesized within different environmental stresses and following incubation with bactericidal concentrations of antibiotics most likely belong to cellular pathways that promote bacterial persistence and are associated with a tolerance phenotype of MAH. To test the concept, we selected MAH lipoprotein LprB synthesized 1.87- and 3.63-fold greater in CLA and AMK treated experimental groups and 1.3-fold higher in the anaerobic condition than in the MAH of biofilm phenotype. Due to the fact that *M. tuberculosis* LprB has been demonstrated to be essential for virulence and survival *in vivo*, we overexpressed the protein in MAH using the pMV261 vector under hsp60 constitutive promoter. The LprB overexpressed clone was tested for *in vitro* antibiotic killing kinetics, biofilm formation assay and for the ability

to invade human macrophages (Figure 2.9). The killing curves for MAH control and LprB experimental clone were established for over 4 days of exposure to AMK and CLA. *In vitro* bacterial killing kinetics for $3x10^5$ bacteria/ml shows increased resistance to amikacin and clarithromycin when compared to the MAH control groups (Figure 2.9A). While both antibiotics had significant bactericidal activity against the wild type and decreasing MAH viability with 5-log by CLA and 6-log by AMK, the overexpression of LprB resulted in bacterial tolerance and decreased MAH viability only 0.5-fold in AMK and 2-log in CLA treatment groups. We did not observe any significant changes in biofilm formation between MAH wild type and LprB clone either in presence or absence of amikacin (Figure 2.9B). In addition, our results demonstrate that by overexpressing the LprB in MAH104, the pathogen is not phagocytosized by human macrophages as effectively as the wild type strain containing the empty plasmid. The time dependent invasion assay shows significant differences between the uptake of LprB and the wild type control over time (Figure 2.9D).

Using the fluorescent RFP control construct of MAH and pMV261:LprB:RFP overexpressing clone, we observe that LprB protein localizes to the bacterial cell surface (Figure 2.9D) and is found in the soluble and insoluble fraction of MAH (Figure 2.9E(1)). Bacteria expressing recombinant protein were mechanically disrupted and soluble total protein fraction was extracted. Protein remaining in the insoluble fraction was extracted in a denaturing buffer containing urea. Protein fractions were separated via SDS-PAGE and analyzed by Western blot to determine the solubility of the RFP and LprB protein constructs. The results indicate that the full length LprB:RFP is accessible from the soluble and insoluble fractions, whereas RFP control localizes primarily to the soluble fraction. In addition, by extracting and analyzing the biofilm biomass for LprB presence busing the western blotting, we demonstrate that MAH lipoprotein localizes into the biofilm matrix (Figure 2.9E(2)).

Conclusions

Mycobacterium avium subsp. *hominissuis* is the most common intracellular pathogen associated with disseminated infection in patients with HIV/AIDS [12]. Individuals with pre-existing chronic lung diseases, such as cystic fibrosis, bronchiectasis and emphysema, and patients who are receiving immunosuppressive therapy, are also predisposed to pulmonary MAH infection [2]. Despite recent advancements in the discovery of new anti-mycobacterial compounds and development of novel delivery methods to quickly achieve the bactericidal concentrations in infected sites and tissues, it is still major challenge to efficiently eliminate infecting organism [6]. The action of antibiotics against mycobacteria is more complex than initially thought. Recent studies on *M. tuberculosis* and on MAH (this study) have shown that although antibiotics are employed at bactericidal concentrations, aiming to kill the pathogen, bacteria viability is still not affected in a significant manner for several days [59].

The adherence to the lengthy therapy is a crucial component for treatment of diseases caused by mycobacterial pathogens. The reasons for the extended treatment are complex and reflect the inability of current antimicrobials to clear phenotypic heterogeneous bacteria quickly, particularly, the subpopulation of susceptible but drug-tolerant bacilli where the persistent fitness to anti-mycobacterial drugs is in fact stimulated and enhanced by the host environmental stresses. In order to enhance MAH killing and eliminate bacteria in different metabolic states (drug-tolerance phenotype) where current antimicrobials are ineffective, a rational therapy needs to be developed. This strategy aims to: 1) identify global proteomic remodeling of MAH within the specific niche of different environmental conditions of the host with and without antibiotic treatments, 2) determine and then 3) target significant bacterial pathways associated with the MAH tolerant/persistent phenotype.

It is widely accepted hypothesis that in order to overcome unfavorable environmental conditions, killing effects of antimicrobials as well as maintain the non-replicate state of infection (linked with tolerance state of the pathogen), bacteria may require expression and synthesis of specific subsets of proteins, which play important roles in “persistence” adaptations and long-term survival. To test this hypothesis, we

investigated the relative protein quantitative analysis of MAH proteome under aerobic, anaerobic and biofilm conditions with and without exposure to antimicrobials using Tandem Mass Tag Mass Spectrometry approach. This study establishes several MAH proteins significantly synthesized within different environmental stresses and following incubation with bactericidal concentrations of antibiotics, and they belong to common metabolic pathways. The identified cellular processes are widely demonstrated in the literature to be associated with mycobacterial metabolic shift and, consequently, promoting drug-tolerance state and pathogen's survival. In addition, the regulation of certain virulence related factor such as LprB associated with aminoglycoside resistance and decreased macrophage uptake can become a possible anti-MAH target.

The phenotypic changes induced by environmental conditions as well as by the presence of antibiotics may have an impact in the ability of the host to defend against the pathogen. Our findings reported here add important information on MAH response to therapy, filling some of the gap on the basic understanding how this pathogen respond to different host environments and drug treatments.

Figures

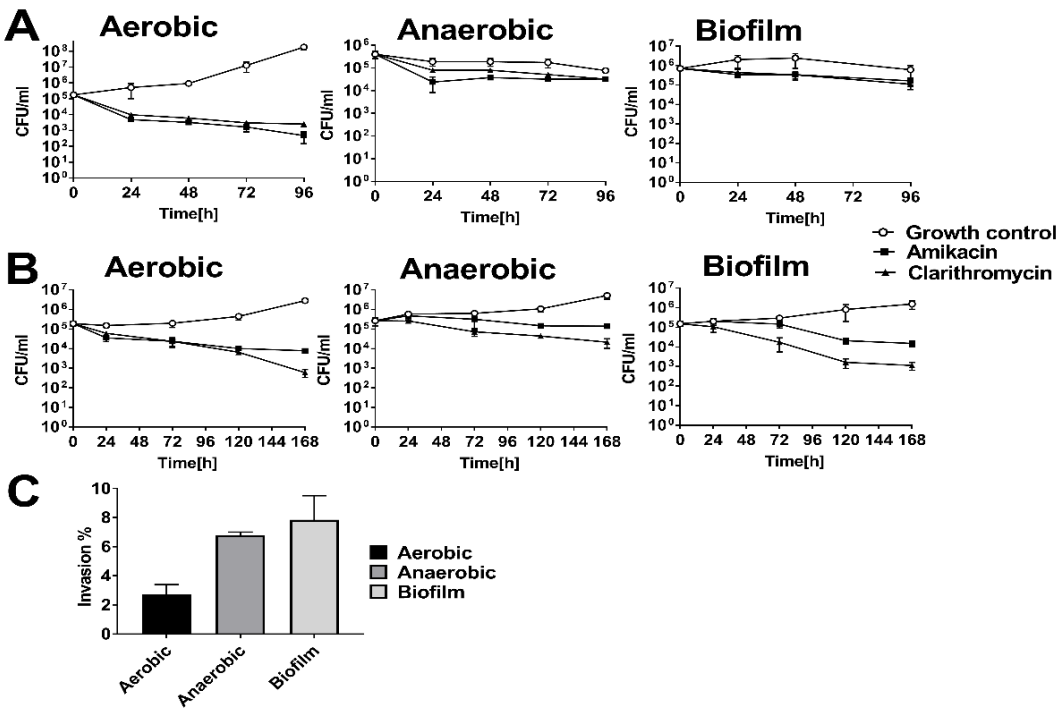

Figure 2.1: MAH killing dynamics *in vitro* and in macrophages. (A) MAH 104 time-kill curves of bactericidal concentrations of AMK and CLA show bacterial CFUs over 4 days in aerobic, anaerobic and biofilm conditions. Antimicrobials were added to the 7H9 Middlebrook liquid medium at time zero and bacterial CFUs were compared with the growth control without the drug treatment. **(B)** MAH104 survival rates in THP-1 macrophages. THP-1 monolayers were infected with bacteria of the aerobic, anaerobic or biofilm phenotype and killing dynamics were recorded over 7 days during AMK or CLA treatment. Bactericidal concentrations of antimicrobials were added to the tissue culture after 2 h infection and then every alternate day. Growth control without drug treatment is also shown. **(C)** MAH104 invasion rates in THP-1 macrophages. Bacteria of the anaerobic and biofilm phenotypes had increased uptake by THP-1 cells when compared to MAH of the aerobic phenotype. MAH were incubated with THP-1 cells for 2 h, extracellular bacteria were removed, and macrophages were lysed for CFU counts. The percentage of invasion was established by calculating the number of bacteria (from inoculum) that entered host cells during 2h infection.

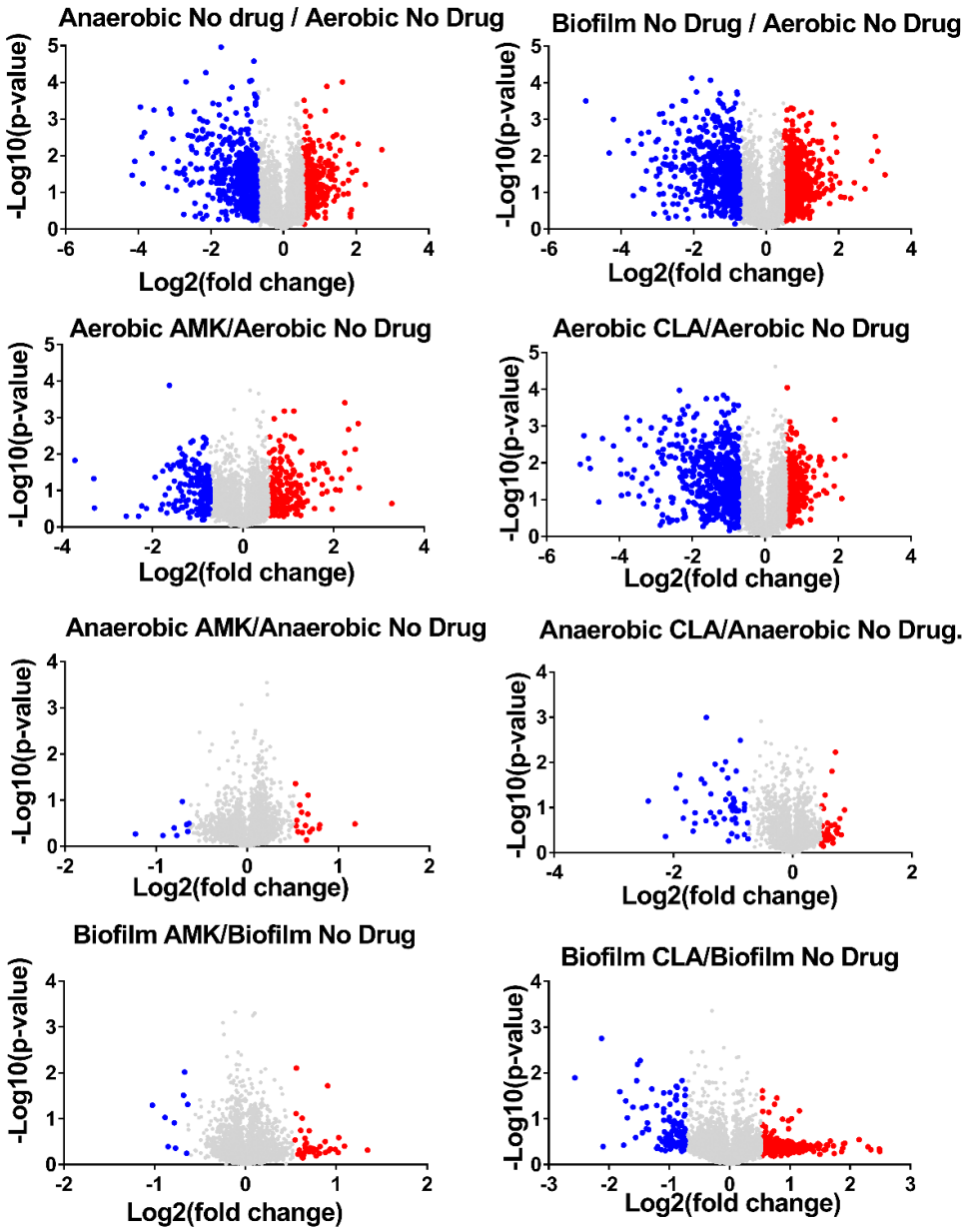

Figure 2.2: **Volcano plots showing proteins that are induced or repressed.** Proteins with upregulation ≥1.5 fold in red and with downregulation ≤1.5 in blue; each dot is one protein. The volcano plot shows the log2-fold changes in gene expression induced by anaerobic and biofilm conditions as compared with aerobic control. The volcano plot also shows the log2-fold changes in gene expression induced by AMK and CLA after 24-hour exposure to aerobic, anaerobic and biofilm phenotypes. Each condition is compared with the corresponding condition with no drug control.

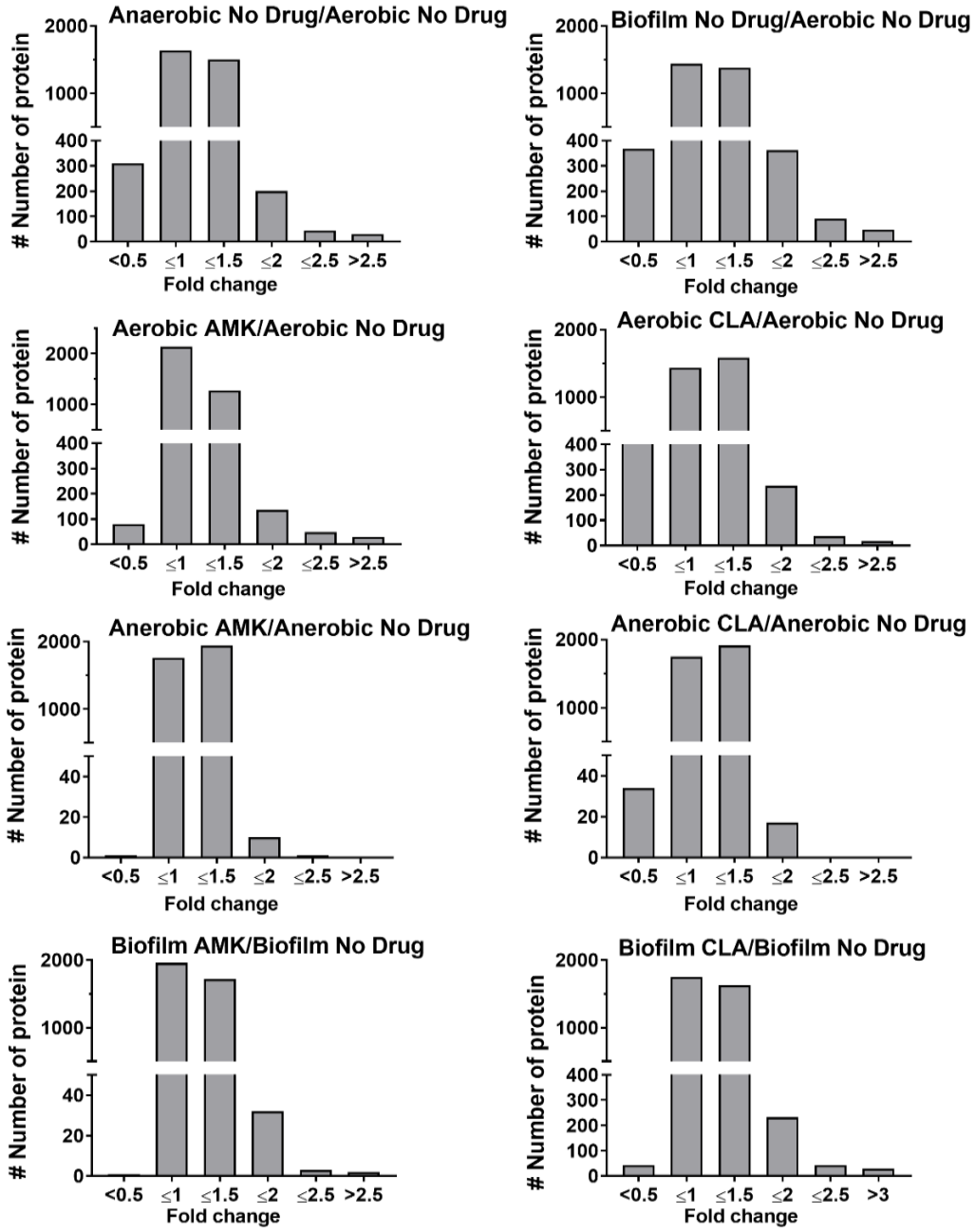

Figure 2.3: Fold changes of differentially expressed MAH proteins. The histograms show the distributions of fold changes of differentially expressed proteins in anaerobic and biofilm conditions with and without AMK and CLA treatments.

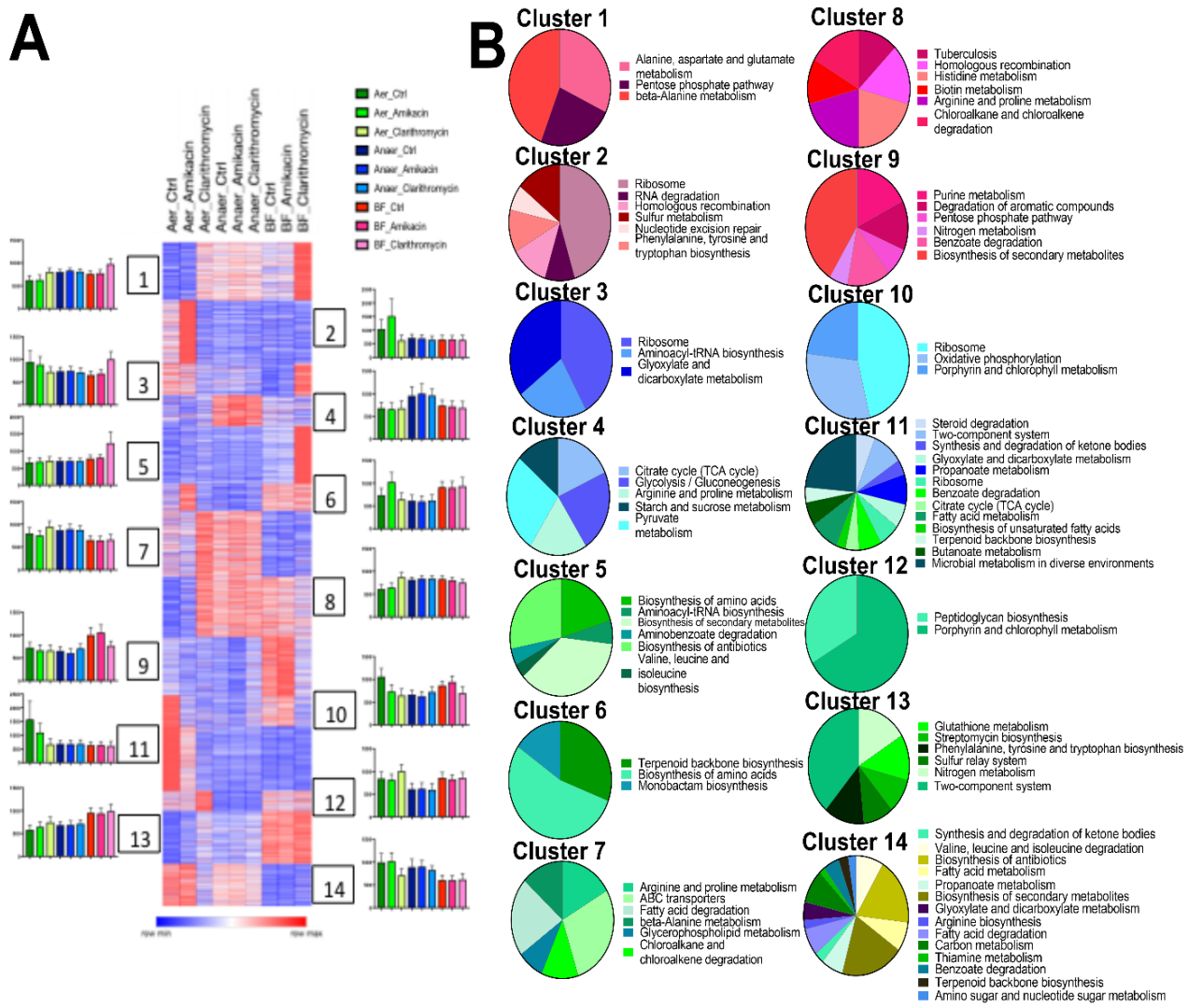

Figure 2.4: The heatmap and clustering analysis for metabolic pathways. (A) Heatmap of K-means clustering have identified groups of proteins with various expression in different treatment groups. The heat map color codes reflect a change. K-means clustering was performed for 3,963 protein-coding genes across all studied groups (adjusted p-value < 0.05). The model-based optimal number of K = 14 was determined. **(B)** Fourteen Pie charts present the KEGG enrichment analysis for metabolic pathways and correspond to 14 clusters.

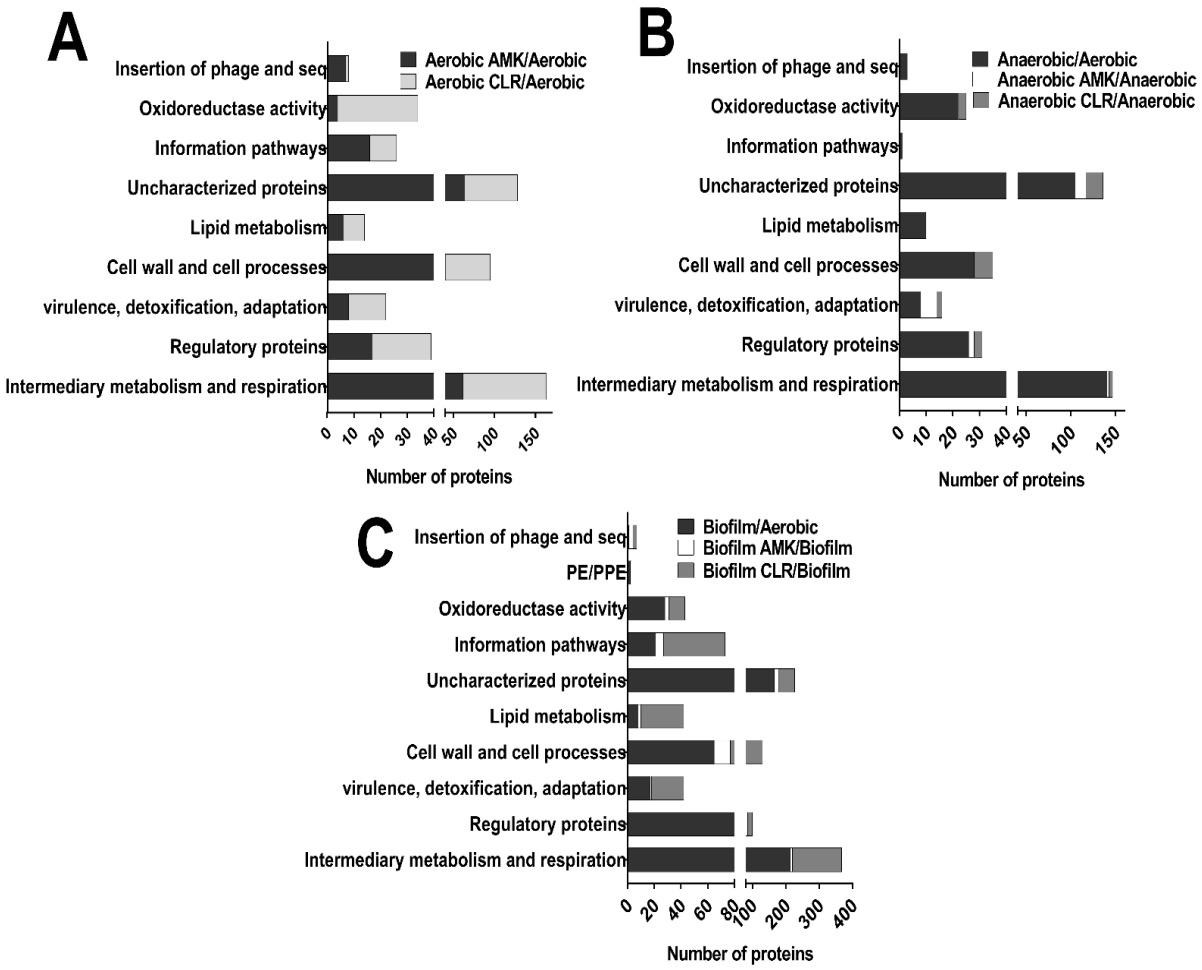

Figure 2.5: Functional classification of MAH upregulated proteins into categories was done by finding the protein homologs of H37Rv strain of *Mycobacterium tuberculosis* and using the functional categorization available on TubercuList webserver of Institute Pasteur or based on predicted or known function for those MAH proteins that do not match to any proteins of H37Rv strain. The histogram shows number of proteins belonging to each functional category

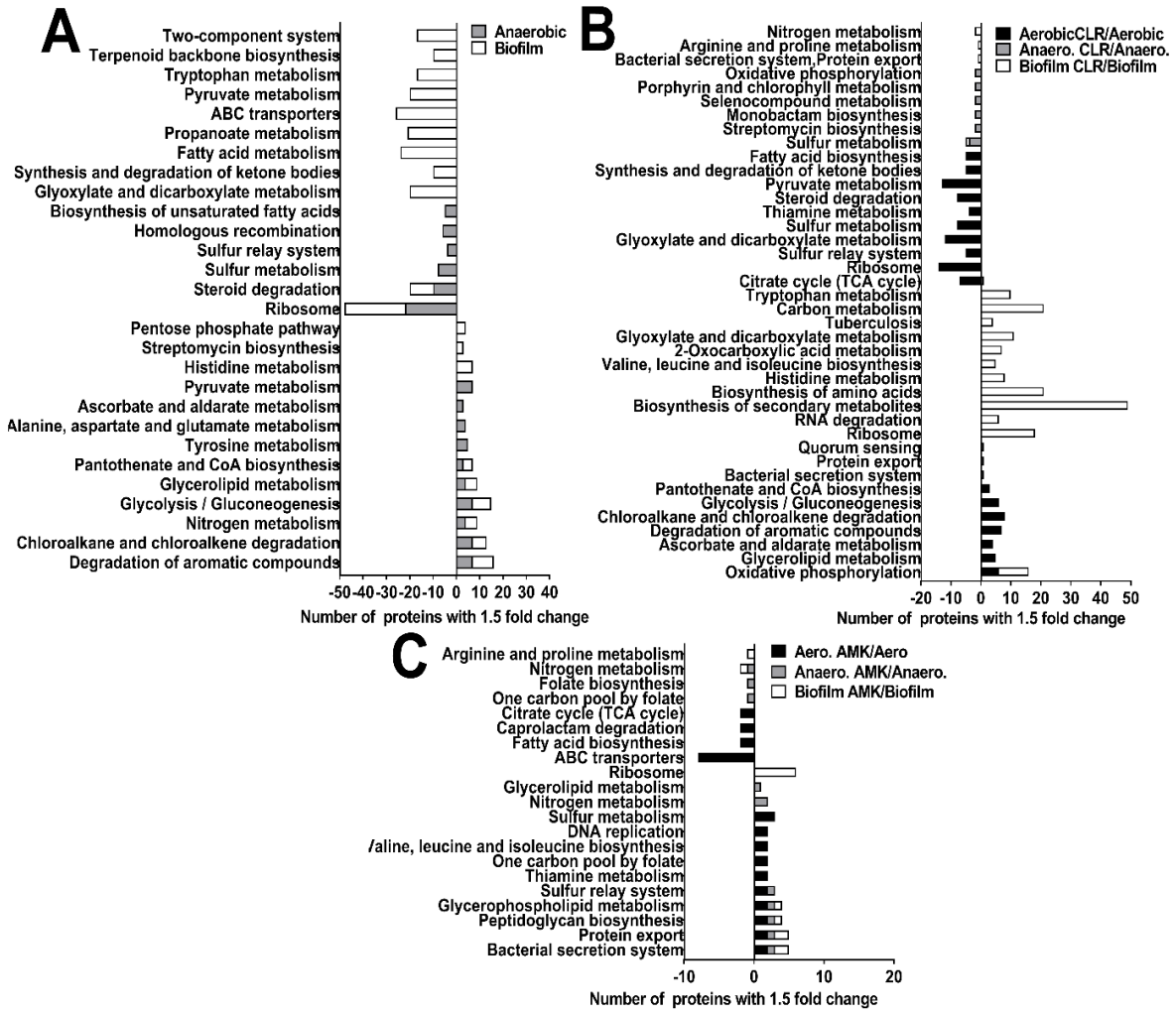

Figure 2.6: MAH metabolic pathway enrichment. Proteins are grouped based on the KEGG pathway database for expressed and downregulated proteins in **(A)** anaerobic and biofilm, **(B)** CLA treatment aerobic, anaerobic and biofilm, and **(C)** AMK treatment aerobic, anaerobic and biofilm groups.

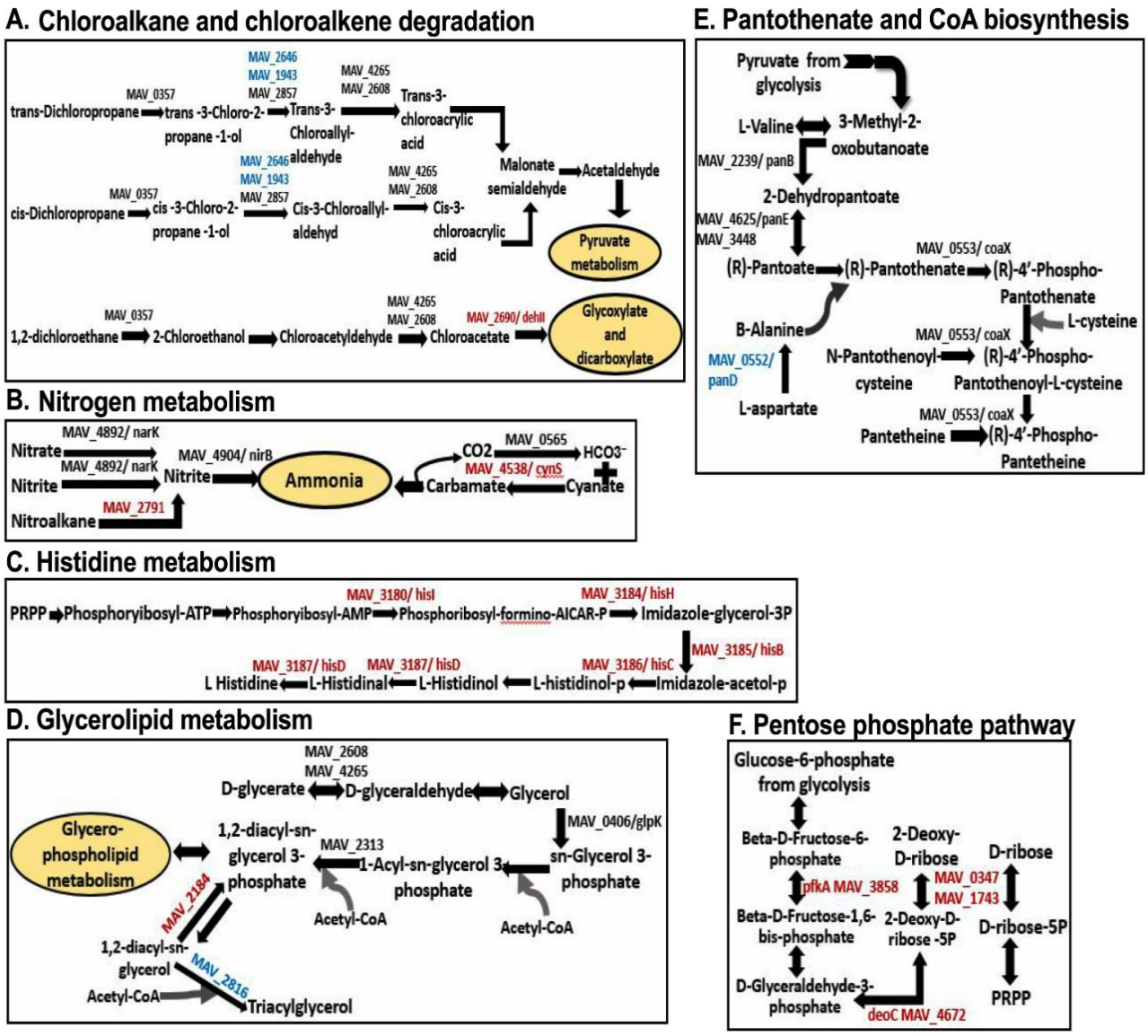

Figure 2.7: Upregulated metabolic pathways of MAH in anaerobic and biofilm conditions. Bacterial proteins synthesized during biofilm formation are presented in red, during anaerobic condition in blue and in both conditions in black

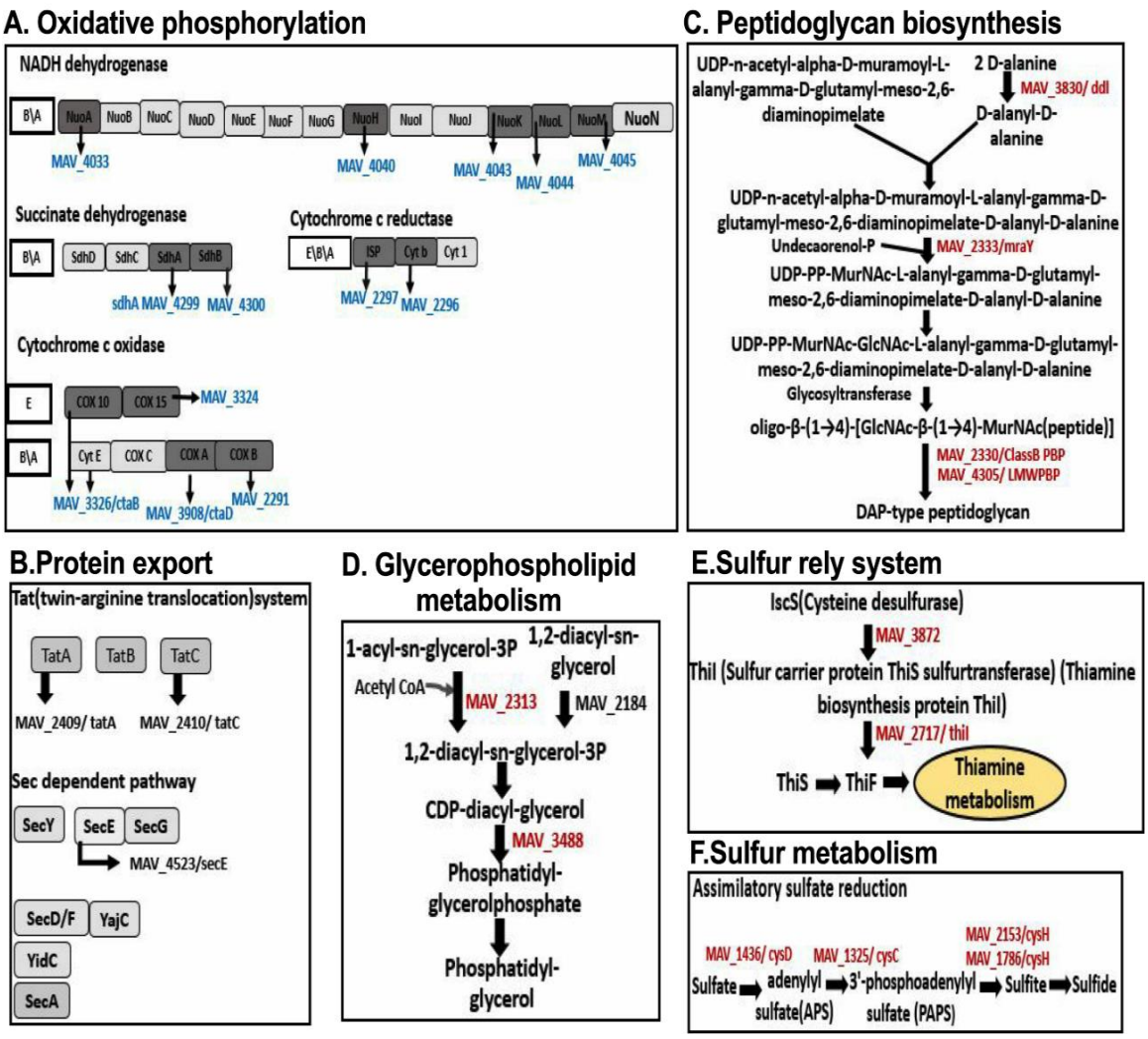

Figure 2.8: Upregulated metabolic pathways of MAH in aerobic, anaerobic and biofilm conditions when exposed to bactericidal concentrations of amikacin and clarithromycin for 24h. Bacterial proteins synthesized in all tested conditions during CLA treatment are presented in blue, during AMK treatment in red and in both drug-groups in black.

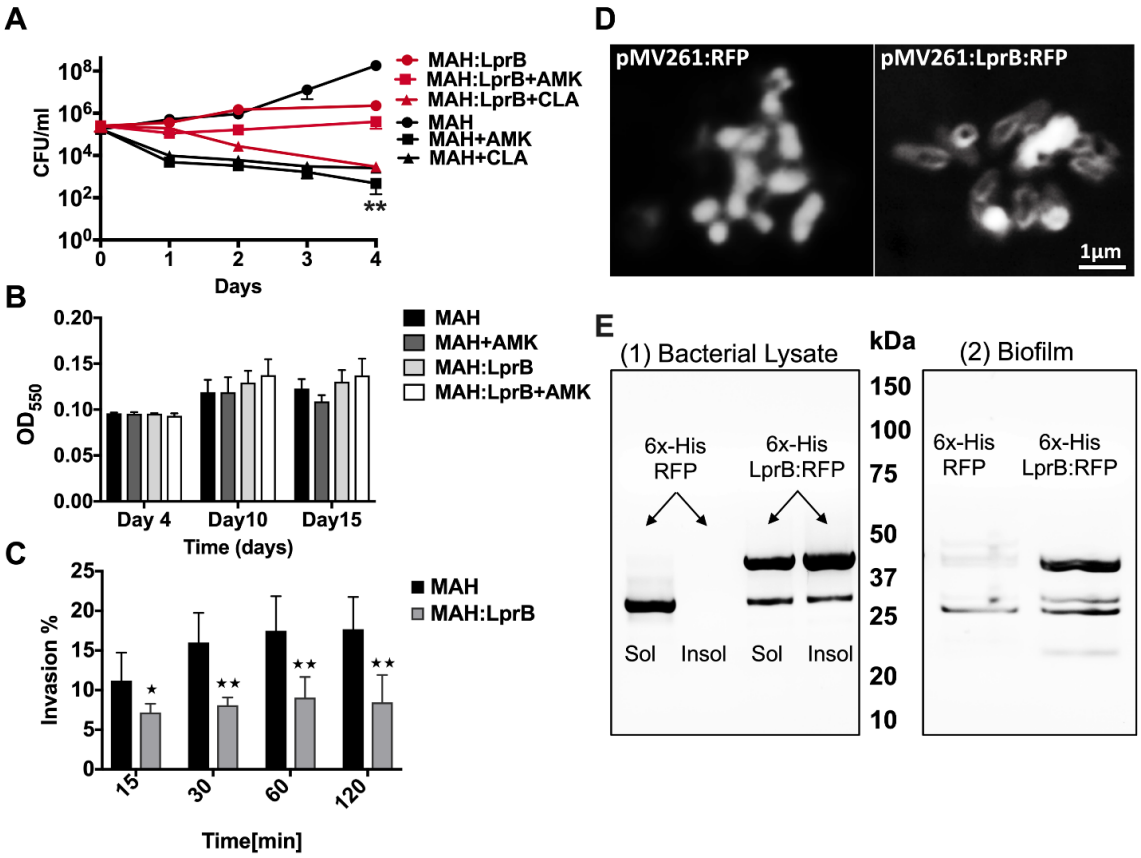

Figure 2.9: (A) *In vitro* time-kill curves for MAH LprB overexpressed clone with and without exposure to bactericidal concentrations of AMK and CLA over 4 days. Results represent means ± standard errors of three independent experiments. **(B)** MAH control and LprB overexpression clones (3×10^8 CFU/ml) were inoculated in PVC 96-well plates with HBSS for 15 days in presence or absence of AMK. The biofilm was evaluated using crystal violet stain as described in Materials and Methods. The *A*570 readings from three experiments are shown and values are means ± standard deviations. **(C)** The time dependent phagocytosis assay of MAH by THP-1 macrophages shows significant differences between the uptake of LprB overexpression clone and the wild type control over time. The experiment was performed in triplicate, repeated three times and means ± SDs were determined. The significance between control and experimental groups is **p<0.01. **(D)** The visualization of RFP fusion LprB protein by fluorescent microscopy, in contrast to MAH control expressing only RFP. **(E)** Western blot analysis of soluble and insoluble fractions of MAH expressing 6X-His tagged proteins. Soluble proteins were first extracted by mechanical disruption in HBSS.

Insoluble proteins were then extracted in a denaturing urea solution. Cell envelope and membrane localizing proteins tend to remain insoluble in HBSS, while cytoplasmic and secreted proteins are readily extracted in HBSS. (1) Cell fractionation shows that LprB protein is found in the insoluble and soluble fraction of MAH, while RFP protein remains only in soluble portion. (2) Biofilms were formed in HBSS at 37°C for 7 days. Supernatants were gently removed and total proteins of the biofilm biomass were extracted in HBSS. In contrast to MAH control expressing only RFP, we observe that LprB lipoprotein is translocated into the MAH biofilm matrix.

References

1. Rindi L, Garzelli C: **Genetic diversity and phylogeny of Mycobacterium avium.** *Infect Genet Evol* 2014, **21:**375-383.

2. Field SK, Fisher D, Cowie RL: **Mycobacterium avium complex pulmonary disease in patients without HIV infection.** *Chest* 2004, **126:**566-581.

3. Goring SM, Wilson JB, Risebrough NR, Gallagher J, Carroll S, Heap KJ, Obradovic M, Loebinger MR, Diel R: **The cost of Mycobacterium avium complex lung disease in Canada, France, Germany, and the United Kingdom: a nationally representative observational study.** *BMC Health Serv Res* 2018, **18:**700.

4. Wallace RJ, Jr., Brown-Elliott BA, McNulty S, Philley JV, Killingley J, Wilson RW, York DS, Shepherd S, Griffith DE: **Macrolide/Azalide therapy for nodular/bronchiectatic mycobacterium avium complex lung disease.** *Chest* 2014, **146:**276-282.

5. Kasperbauer SH, Daley CL: **Diagnosis and treatment of infections due to Mycobacterium avium complex.** *Semin Respir Crit Care Med* 2008, **29:**569-576.

6. Kim EY, Chi SY, Oh IJ, Kim KS, Kim YI, Lim SC, Kim YC, Kwon YS: **Treatment outcome of combination therapy including clarithromycin for Mycobacterium avium complex pulmonary disease.** *Korean J Intern Med* 2011, **26:**54-59.

7. Kwak N, Park J, Kim E, Lee CH, Han SK, Yim JJ: **Treatment Outcomes of Mycobacterium avium Complex Lung Disease: A Systematic Review and Meta-analysis.** *Clin Infect Dis* 2017, **65:**1077-1084.

8. Archuleta RJ, Yvonne Hoppes P, Primm TP: **Mycobacterium avium enters a state of metabolic dormancy in response to starvation.** *Tuberculosis (Edinb)* 2005, **85:**147-158.

9. Lewis AH, Falkinham JO, 3rd: **Microaerobic growth and anaerobic survival of Mycobacterium avium, Mycobacterium intracellulare and Mycobacterium scrofulaceum.** *Int J Mycobacteriol* 2015, **4:**25-30.

10. McNabe M, Tennant R, Danelishvili L, Young L, Bermudez LE: **Mycobacterium avium ssp. hominissuis biofilm is composed of distinct phenotypes and influenced by the presence of antimicrobials.** *Clin Microbiol Infect* 2011, **17:**697-703.

11. Faria S, Joao I, Jordao L: **General Overview on Nontuberculous Mycobacteria, Biofilms, and Human Infection.** *J Pathog* 2015, **2015:**809014.

12. Corti M, Palmero D: **Mycobacterium avium complex infection in HIV/AIDS patients.** *Expert Rev Anti Infect Ther* 2008, **6:**351-363.

13. Bermudez LE, Inderlied CB, Kolonoski P, Wu M, Aralar P, Young LS: **Telithromycin is active against Mycobacterium avium in mice despite lacking significant activity in standard in vitro and macrophage assays and is associated with low frequency of resistance during treatment.** *Antimicrob Agents Chemother* 2001, **45:**2210-2214.

14. Haas W, Faherty BK, Gerber SA, Elias JE, Beausoleil SA, Bakalarski CE, Li X, Villen J, Gygi SP: **Optimization and use of peptide mass measurement accuracy in shotgun proteomics.** *Mol Cell Proteomics* 2006, **5:**1326-1337.

15. Lapek JD, Jr., Mills RH, Wozniak JM, Campeau A, Fang RH, Wei X, van de Groep K, Perez-Lopez A, van Sorge NM, Raffatellu M, et al: **Defining Host Responses during Systemic Bacterial Infection through Construction of a Murine Organ Proteome Atlas.** *Cell Syst* 2018, **6:**579-592 e574.

16. Tolonen AC, Haas W: **Quantitative proteomics using reductive dimethylation for stable isotope labeling.** J Vis Exp. 2014 Jul 1;(89).

17. McAlister GC, Huttlin EL, Haas W, Ting L, Jedrychowski MP, Rogers JC, Kuhn K, Pike I, Grothe RA, Blethrow JD, Gygi SP: **Increasing the multiplexing capacity of TMTs using reporter ion isotopologues with isobaric masses.** *Anal Chem* 2012, **84:**7469-7478.

18. Thompson A, Schafer J, Kuhn K, Kienle S, Schwarz J, Schmidt G, Neumann T, Johnstone R, Mohammed AK, Hamon C: **Tandem mass tags: a novel quantification strategy for comparative analysis of complex protein mixtures by MS/MS.** *Anal Chem* 2003, **75:**1895-1904.

19. Wang Y, Yang F, Gritsenko MA, Wang Y, Clauss T, Liu T, Shen Y, Monroe ME, Lopez-Ferrer D, Reno T, et al: **Reversed-phase chromatography with multiple fraction concatenation strategy for proteome profiling of human MCF10A cells.** *Proteomics* 2011, **11:**2019-2026.

20. Eng JK, McCormack AL, Yates JR: **An approach to correlate tandem mass spectral data of peptides with amino acid sequences in a protein database.** *J Am Soc Mass Spectrom* 1994, **5:**976-989.

21. Elias JE, Gygi SP: **Target-decoy search strategy for increased confidence in large-scale protein identifications by mass spectrometry.** *Nat Methods* 2007, **4:**207-214.

22. Elias JE, Haas W, Faherty BK, Gygi SP: **Comparative evaluation of mass spectrometry platforms used in large-scale proteomics investigations.** *Nat Methods* 2005, **2:**667-675.

23. Peng J, Elias JE, Thoreen CC, Licklider LJ, Gygi SP: **Evaluation of multidimensional chromatography coupled with tandem mass spectrometry (LC/LC-MS/MS) for large-scale protein analysis: the yeast proteome.** *J Proteome Res* 2003, **2:**43-50.

24. Rose SJ, Babrak LM, Bermudez LE: **Mycobacterium avium Possesses Extracellular DNA that Contributes to Biofilm Formation, Structural Integrity, and Tolerance to Antibiotics.** *PLoS One* 2015, **10:**e0128772.

25. Gould TA, van de Langemheen H, Munoz-Elias EJ, McKinney JD, Sacchettini JC: **Dual role of isocitrate lyase 1 in the glyoxylate and methylcitrate cycles in Mycobacterium tuberculosis.** *Mol Microbiol* 2006, **61:**940-947.

26. Bhusal RP, Bashiri G, Kwai BXC, Sperry J, Leung IKH: **Targeting isocitrate lyase for the treatment of latent tuberculosis.** *Drug Discov Today* 2017, **22:**1008-1016.

27. Liu Y, Zhou S, Deng Q, Li X, Meng J, Guan Y, Li C, Xiao C: **Identification of a novel inhibitor of isocitrate lyase as a potent antitubercular agent against both active and non-replicating Mycobacterium tuberculosis.** *Tuberculosis (Edinb)* 2016, **97:**38-46.

28. Gengenbacher M, Rao SP, Pethe K, Dick T: **Nutrient-starved, non-replicating Mycobacterium tuberculosis requires respiration, ATP synthase and isocitrate lyase for maintenance of ATP homeostasis and viability.** *Microbiology* 2010, **156:**81-87.

29. Boshoff HI, Barry CE, 3rd: **Tuberculosis - metabolism and respiration in the absence of growth.** *Nat Rev Microbiol* 2005, **3:**70-80.

30. Wayne LG, Hayes LG: **An in vitro model for sequential study of shiftdown of Mycobacterium tuberculosis through two stages of nonreplicating persistence.** *Infect Immun* 1996, **64:**2062-2069.

31. Wayne LG, Lin KY: **Glyoxylate metabolism and adaptation of Mycobacterium tuberculosis to survival under anaerobic conditions.** *Infect Immun* 1982, **37:**1042-1049.

32. Khan A, Sarkar D: **Nitrate reduction pathways in mycobacteria and their implications during latency.** *Microbiology* 2012, **158:**301-307.

33. Gouzy A, Poquet Y, Neyrolles O: **Nitrogen metabolism in Mycobacterium tuberculosis physiology and virulence.** *Nat Rev Microbiol* 2014, **12:**729-737.

34. Vital-Lopez FG, Reifman J, Wallqvist A: **Biofilm Formation Mechanisms of Pseudomonas aeruginosa Predicted via Genome-Scale Kinetic Models of Bacterial Metabolism.** *PLoS Comput Biol* 2015, **11:**e1004452.

35. Rebora K, Laloo B, Daignan-Fornier B: **Revisiting purine-histidine cross-pathway regulation in Saccharomyces cerevisiae: a central role for a small molecule.** *Genetics* 2005, **170:**61-70.

36. Hove-Jensen B, Andersen KR, Kilstrup M, Martinussen J, Switzer RL, Willemoes M: **Phosphoribosyl Diphosphate (PRPP): Biosynthesis, Enzymology, Utilization, and Metabolic Significance.** *Microbiol Mol Biol Rev* 2017, **81**.

37. Cabral MP, Soares NC, Aranda J, Parreira JR, Rumbo C, Poza M, Valle J, Calamia V, Lasa I, Bou G: **Proteomic and functional analyses reveal a unique lifestyle for Acinetobacter baumannii biofilms and a key role for histidine metabolism.** *J Proteome Res* 2011, **10:**3399-3417.

38. Xu CG, Yang YB, Zhou YH, Hao MQ, Ren YZ, Wang XT, Chen JQ, Muhammad I, Wang S, Liu D, et al: **Comparative Proteomic Analysis Provides insight into the Key Proteins as Possible Targets Involved in Aspirin Inhibiting Biofilm Formation of Staphylococcus xylosus.** *Front Pharmacol* 2017, **8:**543.

39. Zhou YH, Xu CG, Yang YB, Xing XX, Liu X, Qu QW, Ding WY, Bello-Onaghise G, Li YH: **Histidine Metabolism and IGPD Play a Key Role in Cefquinome Inhibiting Biofilm Formation of Staphylococcus xylosus.** *Front Microbiol* 2018, **9:**665.

40. Parish T: **Starvation survival response of Mycobacterium tuberculosis.** *J Bacteriol* 2003, **185:**6702-6706.

41. Leonardi R, Jackowski S: **Biosynthesis of Pantothenic Acid and Coenzyme A.** *EcoSal Plus* 2007, Apr; 2(2): 10.1128/ecosalplus.3.6.3.4.

42. Gengenbacher M, Kaufmann SH: **Mycobacterium tuberculosis: success through dormancy.** *FEMS Microbiol Rev* 2012, **36:**514-532.

43. Zheng R, Blanchard JS: **Steady-state and pre-steady-state kinetic analysis of Mycobacterium tuberculosis pantothenate synthetase.** *Biochemistry* 2001, **40:**12904-12912.

44. Sambandamurthy VK, Wang X, Chen B, Russell RG, Derrick S, Collins FM, Morris SL, Jacobs WR, Jr.: **A pantothenate auxotroph of Mycobacterium tuberculosis is highly attenuated and protects mice against tuberculosis.** *Nat Med* 2002, **8:**1171-1174.

45. Lucarelli AP, Buroni S, Pasca MR, Rizzi M, Cavagnino A, Valentini G, Riccardi G, Chiarelli LR: **Mycobacterium tuberculosis phosphoribosylpyrophosphate synthetase: biochemical features of a crucial enzyme for mycobacterial cell wall biosynthesis.** *PLoS One* 2010, **5:**e15494.

46. Sohaskey CD: **Nitrate enhances the survival of Mycobacterium tuberculosis during inhibition of respiration.** *J Bacteriol* 2008, **190:**2981-2986.

47. Cook GM, Hards K, Vilcheze C, Hartman T, Berney M: **Energetics of Respiration and Oxidative Phosphorylation in Mycobacteria.** *Microbiol Spectr* 2014, Jun; 2(3): 10.1128/microbiolspec.MGM2-0015-2013.

48. Black PA, Warren RM, Louw GE, van Helden PD, Victor TC, Kana BD: **Energy metabolism and drug efflux in Mycobacterium tuberculosis.** *Antimicrob Agents Chemother* 2014, **58:**2491-2503.

49. Matsoso LG, Kana BD, Crellin PK, Lea-Smith DJ, Pelosi A, Powell D, Dawes SS, Rubin H, Coppel RL, Mizrahi V: **Function of the cytochrome bc1-aa3 branch of the respiratory network in mycobacteria and network adaptation occurring in response to its disruption.** *J Bacteriol* 2005, **187:**6300-6308.

50. Jarlier V, Nikaido H: **Mycobacterial cell wall: structure and role in natural resistance to antibiotics.** *FEMS Microbiol Lett* 1994, **123:**11-18.

51. Nguyen L, Thompson CJ: **Foundations of antibiotic resistance in bacterial physiology: the mycobacterial paradigm.** *Trends Microbiol* 2006, **14:**304-312.

52. Nikaido H: **Preventing drug access to targets: cell surface permeability barriers and active efflux in bacteria.** *Semin Cell Dev Biol* 2001, **12:**215-223.

53. Kotera M, Bayashi T, Hattori M, Tokimatsu T, Goto S, Mihara H, Kanehisa M: **Comprehensive genomic analysis of sulfur-relay pathway genes.** *Genome Inform* 2010, **24:**104-115.

54. Hatzios SK, Bertozzi CR: **The regulation of sulfur metabolism in Mycobacterium tuberculosis.** *PLoS Pathog* 2011, **7:**e1002036.

55. Kessler D: **Enzymatic activation of sulfur for incorporation into biomolecules in prokaryotes.** *FEMS Microbiol Rev* 2006, **30:**825-840.

56. Lauhon CT, Kambampati R: **The iscS gene in Escherichia coli is required for the biosynthesis of 4-thiouridine, thiamin, and NAD.** *J Biol Chem* 2000, **275:**20096-20103.

57. Kambampati R, Lauhon CT: **Evidence for the transfer of sulfane sulfur from IscS to ThiI during the in vitro biosynthesis of 4-thiouridine in Escherichia coli tRNA.** *J Biol Chem* 2000, **275:**10727-10730.

58. Paritala H, Carroll KS: **New targets and inhibitors of mycobacterial sulfur metabolism.** *Infect Disord Drug Targets* 2013, **13:**85-115.

59. Danelishvili L, Shulzhenko N, Chinison JJJ, Babrak L, Hu J, Morgun A, Burrows G, Bermudez LE: **Mycobacterium tuberculosis Proteome Response to Antituberculosis Compounds Reveals Metabolic "Escape" Pathways That Prolong Bacterial Survival.** *Antimicrob Agents Chemother* 2017, Jul; 61(7): e00430-17

Chapter 3

Analysis of *Mycobacterium abscessus* subsp. *abscessus* proteome upon exposure to stress conditions reveals common response among pathogenic mycobacteria

Rajoana Rojony[1], Anaamika Campeau[3], Jacob M. Wozniak[3], David J. Gonzalez[3], L. Danelishvili1,[*] and Luiz E. Bermudez[1,2*]

[1]Department of Biomedical Sciences, Carlson College of Veterinary Medicine, Oregon State University

[2]Department of Microbiology, College of Sciences, Oregon State University

[3]Department of Pharmacology, School of Medicine, Skaggs School of Pharmacy and Pharmaceutical Sciences, University of California San Diego

Manuscript in preparation

Abstract

M. abscessus subsp. abscessus (MAB) is clinically important rapidly growing nontuberculous mycobacteria that are responsible for a wide spectrum of skin and soft tissue diseases, ocular and central nervous system infections, pulmonary infection, bacteremia, among other infections. MAB causes pulmonary infections in patients with an underlying respiratory disease such as bronchiectasis or cystic fibrosis and immunocompromised patients with AIDS. MAB is resistance to many of the available therapy and treatment relies on several antibiotics for 18-24 month. The need for prolonged therapy with multiple drugs is a major challenge of MAB treatment, influencing the development of persistent and drug-resistant infections. The reason why several antibiotics at their bactericidal concentrations take several months to eliminate MAB is currently unknown. To investigate MAB proteome changes under aerobic, anaerobic and biofilm conditions, which are conditions encountered in patient's lungs as well as intracellularly, we performed the relative protein quantitative analysis using Tandem Mass Tag Mass Spectrometry sequencing. Quantitative proteomic analysis identified metabolic variations with the change of phenotypes. MAB was exposed to amikacin (32 μg/ml) and Linezolid (128 μg/ml) under aerobic, anaerobic or biofilm condition for 24h and the response was compared with bacterial proteome expressed only in aerobic, anaerobic or biofilm condition without antimicrobials. Overall, 4,000 proteins were identified across all experimental and control groups. Numerous sets of de novo synthesized proteins belonging to diverse metabolic pathways in both anaerobic and biofilm conditions were found, including glycolysis/gluconeogenesis, citrate cycle (TCA cycle), oxidative phosphorylation, nitrogen metabolism, and glyoxylate and dicarboxylate metabolism, known to be associated with bacterial tolerance in *M. tuberculosis*. Following 24h treatment, the common metabolic pathways observed in anaerobic and biofilm conditions due to both drug is glycerophospholipid metabolism and oxidative phosphorylation. We compared M. abscessus and M. avium subsp. hominissuis (MAH) proteomic response in different condition with or without antimicrobials. In both anaerobic and biofilm conditions MAB and MAH bacteria express metabolic enzymes for oxidative phosphorylation, nitrogen metabolism, biosynthesis of secondary metabolites, peptidoglycan

biosynthesis, glyoxylate, and dicarboxylate metabolism. Our study identified promising metabolic pathways that can provide several novel targets to prevent bacterial tolerance mechanism and, subsequently, potentiate rapid killing of MAB.

Introduction

Mycobacterium abscessus complex is a group of rapidly growing non-tuberculous mycobacteria, ubiquitously found in the environment [1][2]. *M. abscessus* complex is currently divided into 3 subspecies: *M. abscessus* subspecies *abscessus (MAB)*; *M. abscessus* subspecies *massiliense* and *M. abscessus* subspecies *bolletii*. MAB is associated with a wide range of clinical diseases. It causes traumatic contaminated skin injury infection, nonsterile post-surgical soft tissue infection, central nervous system infection, bacteremia, and among other infections [1]. The Organisms of *Mycobacterium abscessus* complex also cause pulmonary infections in patients with underlying respiratory diseases such as bronchiectasis and cystic fibrosis [3]. The incidence and prevalence of patients with nontuberculous mycobacterial (NTM) lung infections are in rising in recent years [4]. Although *M. avium* complex is the most common non-tuberculous mycobacteria (NTM) species responsible for pulmonary disease, MAB is the most antibiotic resistance pathogenic NTM [2][5].

According to recommended current guidelines the treatment of MAB infection, in general, relies on a macrolide-based (clarithromycin or azithromycin) antibiotic therapy combined with intravenous amikacin with cefoxitin or imipenem for several months [3]. In spite of multidrug treatment, usually, the success rate of MAB treatment is only 25% to 42% [6]. The main challenge for treating MAB patients is the intrinsic resistance to antibiotics, and the inability to rapidly kill MAB with multiple compounds even when administered using bactericidal concentrations and for extended duration of treatment[6]. MAB response to antibiotics is incomplete since MAB enters in a nonreplicating persistent state and become tolerant to antibiotics. Like other bacterial biofilm, MAB biofilm also shows minimum response to antibiotics, as biofilm prevents the optimal penetration of antibiotics [7][8]. Evidence suggests that low nutrients, low pH and lack of the oxygen prompt a nonreplicating state in the lung as well as in vitro, by changing the metabolic state of the pathogen and enhance antibiotics resistance [9][10]. MAB can survive for prolonged periods in granuloma (low oxygen condition) in the lung of cystic fibrosis patients by altering their metabolism from aerobic to anaerobic state and by changing their phenotype to biofilm [8][11][12].

The discovery of new treatment approaches is needed to fight against MAB. We sought to fill the gap in knowledge on MAB survival strategies under non-replicating conditions and how does phenotypic change increase bacterial tolerance during exposure with antibiotics. MAB proteome changing under aerobic, anaerobic and biofilm conditions, as well as the response following exposure to bactericidal concentrations of active antimicrobials, were studied. Exposure to linezolid, a member of the synthetic oxazolidinone class, which works by suppressing bacterial protein synthesis. Linezolid is available for the treatment of drug resistance gram-positive bacterial infection [13][14]. Some recent studies suggest that linezolid could be an alternative option for the multidrug resistance tuberculosis treatment [15][16]. Our study findings suggest global proteomic changes in the upregulation and downregulation of many enzymes supporting bacterial survival in non-replicating metabolic state.

Materials and Methods

Mycobacteria strains and culture conditions. *Mycobacterium abscessus subsp. abscessus* strains 19977 is virulent clinical isolate were isolated from patients with either a bacterial infection or a lung infection. Before macrophage infection or in vitro study, organisms were suspended in Hanks' balanced salt solutions (HBSS), and the concentration of the bacterium per milliliter was adjusted with McFarland 0.5 and then plated onto Middlebrook 7H11 agar plates supplemented with 10% oleic acid, albumin, dextrose, and catalase (OADC, Hardy Diagnostics, Santa Maria, CA) to determine the number of bacteria in the inoculum. MAB 19977 was grown at 37°C, until mid-log phase (2-3 days) in 7H9 Middlebrook broth.

Antimicrobial reagents and susceptibility testing. Amikacin was purchased from Sigma-Aldrich and Linezolid from Biomol (SYN-3021). Amikacin and linezolid were solubilized into water and DMSO respectively. Different drug concentrations were obtained by dilution in Hank's balanced salt solution (HBSS).

Antibiotic susceptibility testing was performed with a broth microdilution method. Briefly, 3×10^6 bacteria/ml were seeded in 7H9 Middlebrook broth supplemented with oleic acid, albumin, dextrose, and catalase. The number of bacteria for the inoculum was compared with McFarland 0.5, and confirmed by plating onto 7H10 agar. For every antibiotic susceptibility testing, we used as control 7H9 media without any antibiotics. The concentration of amikacin and linezolid ranged from 0.065 to 256 µg/ml. MAB 19977 bacteria were grown with or without antibiotic in a shaker at 37°C for 3 days. Minimal Inhibitory Concentrations (MICs) were visually determined after day 3. The antibiotic concentration that gives visibly clear or non-turbid media is the MIC of that particular drug. For this study, we determined Minimal Inhibitory Concentrations MBCs by centrifugation of non-turbid media to make bacterial pellet. Pelleted bacteria were suspended into PBS, serially diluted and plated. The plates were incubated at 37°C for 4 days to see the bacterial colony. Drug Concentration that inhibits 99.9% bacterial growth was considered the bactericidal concentration of that particular drug.

Antibiotic killing kinetics *in vitro*. MAB 19977 inoculum was prepared into HBSS. MAB inoculum was compared with McFarland 0.5, took 1ml into 9ml HBSS to make $3x10^7$ bacteria/ml. We took 300µl for 3ml of 7H9 liquid media containing MBCs of the following drugs: AMK, 32µg/ml; LNZ, 128 µg/ml. Samples were taken after 24 h, 48 h, 72h, 96h and 144h of drug exposure and plated onto 7H11 agar plates for CFU determination. For each time point, we kept one growth control tube containing only 7H9 media with bacteria.

To determine the MAB antibiotic killing kinetics in anaerobic conditions in vitro, as mentioned before, we prepared tubes containing $3x10^6$ bacteria/ml with the appropriate amount of antibiotic and growth control without antibiotic. We kept those tubes into anaerobic jars (BD BBL™ GasPak™ Jar), used grease over the rim of the chamber to seal the Jar tightly then kept within shaker at 37°C. Anaerobic indicator (BD BBL™ GasPak™ anaerobic and CO2 indicators) was inserted inside the jar. At each time point, the jar was opened, pulled out tubes and centrifuged at 3600rpm for 20 min. Pellet was resuspended with PBS, serially diluted and plated onto the 7H10-agar plate to count CFU/ml.

Finally, the killing kinetics of MAB by antibiotic was determined under biofilm conditions. Bacterial inoculum was prepared $3x10^7$ in HBSS and 100 microliters were added into each well of a 96 well microtiter plate. The surface was covered with a membrane and kept at 25°C for 7 days. After 7 days the entire supernatant was removed and antibiotic was added into each well. At each time point, bacteria were pulled out and plated to determine the number of viable bacteria. The experiments were carried out in duplicate and repeated three times.

Antibiotics killing kinetics in human macrophage. Human THP-1 cell lines (TIB-202)were obtained from the American Type Culture Collection (Manassas, VA) and cultured in RPMI 1640 medium supplemented with heat-inactivated 10% fetal bovine serum (FBS, Gemini Bio-products, Sacramento, CA), L-glutamine, and 25 mM HEPES (Corning, Manassas, VA) incubated at 37°C and in an atmosphere of 5% CO2.

Intracellular killing assays were performed as previously described, with minor modifications. Briefly, 3×10^5 cells per well were added to a 48-well tissue culture plate and monolayers were treated with 50 ng/ml of phorbol myristate acetate for 24 h to stimulate maturation of the monocyte. MAB 19977 with HBSS was kept in an anaerobic chamber for 24h to express anaerobic phenotype and kept in 25°C for 7 days to express biofilm phenotype. Differentiated macrophage monolayers were infected with MAB aerobic, anaerobic and biofilm phenotypes at a multiplicity of infection (MOI) of 1 bacteria: 1 cell. Infected macrophages were incubated at 37°C and 5% CO2 for 2h. Extracellular bacteria were subsequently removed by washing five times with HBSS and treating the cells with 400 μg/ml amikacin for 30min. Infected monolayers were treated with the above-listed concentration of AMK and LNZ. Infected macrophages without drug treatment served as a control. Media and antibiotics were replaced every other day. Cells were lysed at 2h, day2, day4 day6 followed by plating on 7H11 agar plates to determine the intracellular bacterial CFU.

Sample preparation and proteome analysis. For aerobic and anaerobic study $5x10^8$cells/ml of *M. abscessus* 19977 were inoculated in 50ml of 7H9 culture media with or without drugs. MBC of AMK or LNZ was added to the medium. We kept those tubes into shaker at 37°C for aerobic experiment and kept into an anaerobic jar at 37°C for the anaerobic experiment. The bacteria were exposed to the drugs for 24 hours. For biofilm study, we prepared a $9x10^8$ cells/ml inoculum into 40ml HBSS, compared it with McFarland 3 also measured absorbance at 625nm which was close to 0.38 to 0.42. We kept the flasks at 25°C for 7 days. After 7 days, gently removed the supernatant and added antibiotic and kept for 24 hours. At 24h, all the samples were centrifuged at 3600×g rpm for 20min at 4°C, washed the pellet with PBS and resuspended with 3% SDS containing EDTA-free Protease Inhibitor Cocktail (Sigma-Aldrich) to lyse bacterial cells. Bacterial cells were mechanically disrupted through bead beating 3 times for 40 sec each after each 40-sec bead beating samples were kept in ice. All supernatant fluid was collected, centrifuged at 15000×g rpm for 10 min and passaged through 0.22μm filters. Finally, the protein concentration of different samples was measured with the Thermo Scientific NanoDrop machine.

Tandem Mass Tag (TMT) labeling and Liquid chromatography-mass spectrometry (LC-MS). Precleared lysates were immersed in equal volumes of 8 M urea and a lysis buffer containing 75 mM NaCl, 3% sodium dodecyl sulfate (SDS), 1 mM sodium fluoride, 1 mM beta-glycerophosphate, 1 mM sodium orthovanadate, 10 mM sodium pyrophosphate, 1 mM phenylmethylsulfonyl fluoride, 1X complete EDTA-free protease inhibitor cocktail (Roche), and 50 mM HEPES (Sigma), pH 8.5. Samples were subjected to pulsed probe sonication to ensure complete cell lysis. A pulse protocol of 15 seconds "on" at 20% amplitude was alternated with 15 second periods of rest three times. Disulfide bonds were reduced in 5 mM of dithiothreitol (DTT) for 30 minutes at 56°C. Reduced cysteine residues were alkylated in 15 mM of iodoacetamide (IAA) for 20 minutes in a darkened environment at room temperature. The alkylation reaction was subsequently quenched by the addition of the original added volume of DTT and incubation of the solution in a darkened environment at room temperature for 15 minutes.

Protein was precipitated by adding one-quarter of the total sample volume of trichloroacetic acid (TCA) to the sample solution. Samples were agitated and incubated on ice for 10 minutes before being subjected to centrifugation at 14,000 rpm for 2 minutes. The resultant supernatant was removed and samples kept on ice for the subsequent wash steps. Samples were washed in 300 µL of ice-cold acetone and subjected to centrifugation at 14,000 rpm for 2 minutes. The supernatant was removed and the acetone wash step repeated. After removal of the second acetone wash supernatant, samples were dried on a 56°C heating block. Samples were resuspended in 300 µL of a solution of 1 M urea and 50 mM HEPES, pH=8.5. Resuspended samples were subjected to 5 minutes of vortexing and 5 minutes of water bath sonication. Samples were then subjected to two-step digestion. First, 3 µg of sequencing-grade LysC was added and samples were incubated on a shaker at room temperature overnight. Second, 2.8 µg of sequencing-grade trypsin was added to the samples and were incubated at 37°C for 6 hours. Samples were acidified by the addition of 20 µL of 10% trifluoroacetic acid and were desalted on C18 columns using previously-described methods. Samples were lyophilized at this stage.

Lyophilized samples were immersed in a solution of 50% acetonitrile and 5% formic acid prior to quantification. Peptide quantification was performed using the Pierce Quantitative Colorimetric Peptide Assay (Thermo). 50 µg of each sample was separated for tandem mass tag (TMT) labeling. An internal standard containing an equal mass of each sample was prepared, and 50 µg of the standard was separated per intended set of 10 TMT labels. Sample aliquots designated for further analysis were lyophilized.

Lyophilized samples were resuspended in 50 µL of a solution of 30% anhydrous acetonitrile and 200 mM of HEPES, pH=8.5. TMT labels were resuspended in 40 µL of anhydrous acetonitrile and subjected to vigorous shaking for 5 minutes. A TMT label assignment scheme was generated using two core principles: first, no two experimental replicates were assigned to the same label, and second, each experimental condition was represented in each set of 10 labels. 8 µL of each label was added to the designated sample, and the labeling reaction was allowed to proceed at room temperature for 1 hour. Reaction quenching was performed via the addition of 9 µL of a solution of 5% hydroxylamine and room temperature incubation for 15 minutes. Reactions were acidified through the addition of 50 µL of a solution of 1% TFA. Samples assigned within each set of 10 labels were mixed, and each resulting mixture was desalted on C18 columns using the same methods as above.

Multiplexed samples were subjected to basic reverse phase liquid chromatography on an Ultimate 3000 HPLC with 4.6 mm x 250 mm C18 resin column. Samples were resuspended in 120 µL of a solution of 5% acetonitrile and 5% formic acid and loaded onto the column. Samples were eluted as 96 fractions on a gradient ranging from 5% to 35% acetonitrile in 10 mM ammonium bicarbonate. Fractions were concatenated as described previously, and alternating concatenated fractions were lyophilized (Wang et al., 2011). Lyophilized fractions were resuspended in a solution of 5% acetonitrile and 5% formic acid prior to analysis by LC-MS.

All mass spectrometry-based analysis was performed on an Orbitrap Fusion Tribrid Mass Spectrometer with in-line Easy nLC System at the University of California San Diego

Mass Spectrometry Facility. Samples were loaded onto a column pulled and packed in-house. The inner diameter of the column was 100 µm and the outer diameter was 350 µm. The contents of the column were as follows: the distal tip was packed with 0.5 cm of 5 µm C4 resin followed by 0.5 cm of 3 µm C18 resin. The remaining 29 cm was packed with 1.8 µm C18 packing resin. Peptides were eluted on a 165-minute gradient ranging from 11% to 30% acetonitrile in 0.125% formic acid at a flow rate of 300 nL/min. The column was heated to 60°C.

All data were acquired in centroid mode. Electrospray ionization was achieved through the application of 2000 V of electricity through a T junction connecting sample, waste and column capillaries. MS1 spectra were collected in data-dependent mode using a scan range between 500-1200 m/z with a resolution of 60,000. Automatic gain control was set to 2x105 and the maximum injects time was 100 ms. The top N method for peak selection was selected, with N set to 10 for MS2 and MS3 analysis. Parent ions were selected in the quadrupole at 0.5 Th for MS2 fragmentation. Parent ions were fragmented using collision-induced dissociation (CID) energy and fragment ions were detected in the ion trap with a rapid scan rate automatic gain control of 1x104. TMT reporter ion fragmentation was performed using synchronous precursor selection (SPS). The MS2 precursors chosen were fragmented using high energy collisional dissociation (HCD). Reporter ions were detected in the Orbitrap. The lower limit of detection at the MS3 stage was set to 110 m/z and automatic gain control was set to 1x105. The maximum injects time was 100 ms.

MS data processing. Raw data files were searched using Proteome Discoverer 2.1 using SEQUEST-HT. The reverse database strategy for decoy database generation was used. Files originating from the *M. abscessus* study were searched against the *M. abscessus* ATCC 19977 strain reference proteome downloaded on 11/21/2017. The precursor and fragment ion mass tolerances were set to 50 ppm and 0.6 Da, respectively. The digesting enzyme was specified as trypsin, and up to two missed cleavages were allowed. Peptides of fewer than 6 amino acids or more than 144 amino acids were excluded. Dynamic modification of methionine oxidation (+15.995 Da) was included in the search parameters, as were static modifications for isobaric tandem

mass tags at the N-termini and on lysine residues (+229.163 Da) and carbamidomethylation of cysteine residues (+57.021 Da). Filtering of spectra was performed in Percolator at the peptide and protein levels at a 1% FDR threshold.

Resultant peptide spectral matches were manually filtered to exclude spectra without high confidence, with rejected PSM ambiguity status, with isolation interference larger than 25 and with an average signal to noise value of less than 10. TMT relative abundance values were summed within proteins matches. Data normalization was performed using a two-step process. TMT signal to noise values was first normalized to the pooled internal standard divided by the median of all internal standard values. The resultant values were then normalized to the median signal to noise values for each label divided by the median of all channel median values to account for variable labeling efficiencies.

The identified MAB proteins were classified into several distinct groups, based on their molecular function. This functional classification based on gene ontology was conducted by blasting the amino acid sequence of MAB proteins against the protein sequence database of *M. tuberculosis* strain H37Rv, using the Institute Pasteur's TubercuList web server (http://genolist.pasteur.fr/TubercuList/). The MAB unmatched proteins were classified based on their predicted function or grouped into an uncharacterized class.

Statistical analysis. Statistical significance for binary comparisons was performed on proteomics data using the Student's t-test. The f-test was employed to ensure that the statistical assumption of equal variance required for the Student's t-test was met; if it was not, the Student's t-test with Welch's correction was used. Volcano plots were constructed using GraphPad Prism 7. K means clustering was performed on proteomic datasets using the Morpheus K-means clustering tool (https://software.broadinstitute.org/morpheus/). The appropriate number of clusters was determined using the elbow method.

Experiments were repeated at least three times, and the results are expressed as a mean ± standard deviation. The comparisons among experimental groups were performed

with ANOVA and Student's t-test when appropriate. A p-value of <0.05 was considered to be statistically significant.

Results

The delayed killing of MAB by antimicrobials. We have determined the minimal inhibitory concentration (MIC) using the broth microdilution method. MIC is a drug concentration at which 90% of MAB growth was inhibited. The MIC of AMK and LNZ for MAB was 2μg/ml and 8μg/ml respectively. The bactericidal concentrations for amikacin was 32μg/ml and 128μg/ml for linezolid. The antibiotic killing dynamics were studied in aerobic, anaerobic and biofilm conditions for 6 days (Figure 3.1A). We observed a complete absence of viable bacteria in the aerobic condition after 4 days following AMK and LNZ treatment. A slight decline in MAB CFU/mL was seen for AMK treatment in the anaerobic condition; whereas LNZ could eliminate MAB in anaerobic conditions after 4 days of treatment. No significant change was seen in MAB CFU/mL when biofilms were incubated with either amikacin or linezolid.

MAB survival following exposure to antimicrobials in human macrophages. THP-1 monolayers were infected with MAB expressing either aerobic, anaerobic or biofilm phenotypes. For each phenotype, the bacterial survival rate within macrophages without antimicrobial treatment served as a control. As shown in Figure 3.1C, THP-1 cells had increased uptake of MAB of the biofilm phenotype when compared with uptake rates of aerobic and anaerobic bacteria. Furthermore, under aerobic condition MAB survived in macrophages when exposed to antimicrobials. Even after 7 days of treatment with bactericidal concentrations of antimicrobials, host cells were unable to clear infection (Figure 3.1B) resulting in 2.5 and 3.5-log decrease of intracellular bacteria during AMK and LNZ treatment at day 7, respectively. While MAB of anaerobic condition grew within macrophages similarly as the aerobic bacteria, MAB of biofilm phenotype showed little growth initially within the THP-1 cells without any antibiotic treatment but regained the growth after day 3. Biofilm phenotype of MAB had grown very faster within macrophage than aerobic or anaerobic phenotype. Upon exposure to antibiotics both AMK and LNZ exhibited some killing effects on MAB of both anaerobic and biofilm phenotypes but unable to clear the infection.

Global proteome response of MAB under Aerobic, Anaerobic and Biofilm Conditions and upon Exposure to antimicrobials. To identify changes in MAB proteomics under different conditions, which are encountered within the lung of infected patients. The quantitative TMT Mass Spectrometric sequencing was performed for samples collected at 24 h time point and, overall, 4,000 proteins were identified across all experimental and control groups. The identified protein list along with their normalized spectral counts, annotations and fold changes over control at corresponding time points for each environmental condition and antimicrobial exposure is presented in the supplemental material (Supplemental Table 1). Volcanic plots presented in Figure 3.2 gives a global overview of induced and repressed proteins following bacterial exposure to different environmental conditions and antibiotics. More specifically, while the incubation to anaerobic and biofilm conditions resulted in upregulation of 551 and 866 proteins, 556 and 743 proteins were downregulated when compared to MAB of aerobic condition. Proteome analysis of MAB treated with AMK for 24 h revealed 587, 43, 139 synthesized and 437, 8, 254 downregulated proteins in aerobic, anaerobic and biofilm conditions, respectively, when compared to control no drug treatment group. In the presence of LNZ, 755, 483, 72 proteins were upregulated and 720, 53, 320 proteins were downregulated in aerobic, anaerobic and biofilm conditions, respectively, when compared with only condition controls. Figure 2.3 demonstrate the distribution of the average fold changes for proteins at different environmental conditions with or without drug treatments.

For a global overview of proteomic changes in MAB response to conditions and antibiotics, without exclusively focusing on the induced proteins only, we used Morpheus to identify K-means clustering (Figure 3.4A). We compared protein levels in each drug treatment versus untreated bacteria using an analysis paired by antibiotic and condition. In addition, with the elbow method, we found seven optimal number of clusters. The heat map shows that proteins of clusters one mainly expressed under aerobic condition and cluster 3 expressed under biofilm conditions. Cluster 2 and 6 proteins were expressed more in aerobic conditions due to AMK and LNZ respectively. Pie charts in Figure 3.4B demonstrate metabolic pathway enrichment related to each cluster.

Functional grouping of 1.5-fold and more synthesized MAB proteins. Mass spectrometric analysis of MAB samples found a total of 587 proteins and 755 proteins synthesized 1.5-fold and more during 24h amikacin and linezolid exposure in the aerobic condition. We categorized differentially synthesized MAB proteins into functional groups as described in the methods. Most represented categories in the aerobic condition during MAB exposure to both antibiotics in were intermediate metabolism and respiration (477 proteins), cell wall and cell processes (298 proteins), regulatory proteins (118 proteins), lipid metabolism (107 proteins), virulence, detoxification, adaptation (96 proteins), metabolic enzymes falling into oxidoreductase activity category (72 proteins), information pathway (72 proteins)and majority of proteins with unknown function (234 proteins) (Figure 3.5A).

In the anaerobic condition, 24h exposure to AMK and LNZ resulted in the induction of the synthesis of 43 and 483 protein, respectively. The distribution of represented categories was the following: 4 and 101 proteins of the intermediate metabolism and respiration, 21 and 79 of regulatory proteins, 5 and 15 proteins from the virulence, detoxification, adaptation group, 1 and 19 were enzymes with the oxidoreductase activity, 9 and 88 proteins in cell wall and cell processes, 1 and 19 proteins for information pathway in the anaerobic-AMK and anaerobic-LNZ groups, respectively (Figure 3.5B).

The distribution of represented categories for biofilm-AMK and biofilm-LNZ experimental groups were the following: intermediary metabolism and respiration (26 and 27 proteins), regulatory proteins (28 and 4 proteins), in virulence, detoxification, adaptation (4 and 1 proteins), cell wall and cell processes (33 and 17 proteins), lipid metabolism (8 and 2 proteins), information pathways (11 and 10 proteins), proteins with oxidoreductase activity (6 and 1 proteins), and uncharacterized proteins (51 and 26 proteins) (Figure 3.5C).

While in the anaerobic and biofilm condition, 551 and 866 proteins were upregulated with 1.5-fold more. Most represented categories in the anaerobic and biofilm condition belongs to intermediate metabolism and respiration (227 and 362 proteins), cell wall and cell processes (101 and 155 proteins), regulatory proteins (43 and 92 proteins), lipid metabolism (36 and 40 proteins), virulence, detoxification, adaptation (51 and 49

proteins), metabolic enzymes falling into oxidoreductase activity category (31 and 49 proteins), information pathway (26 and 23 proteins) and some proteins with unknown function (84 and 155 proteins) (Figure 3.5D).

The metabolic pathway enrichment in environmental conditions and drug treatment groups are presented in Figure 3.6. The protein assignment to KEGG metabolic pathways showed several over-represented metabolic categories that are further discussed below.

Characterization of MAB metabolic pathways expressed under environmental conditions: We identified eleven metabolic pathways expressed under the anaerobic condition and thirteen for biofilm condition when compared to the aerobic condition alone (Figure 3.6A). Among them, ten pathways were common between anaerobic and biofilm conditions. The metabolic pathways present in both anaerobic and biofilm conditions are pyruvate metabolism, glycolysis/gluconeogenesis, citrate cycle (TCA cycle), oxidative phosphorylation, carbon metabolism, starch and sucrose metabolism, alanine, aspartate and glutamate metabolism, nitrogen metabolism and glyoxylate and dicarboxylate metabolism.

MAB metabolic pathways expressed under different environmental conditions in the presence of antibiotics: We identified ten metabolic pathways expressed under aerobic condition, eight under anaerobic condition and six under biofilm condition when treated with AMK, and the expression of these pathways in anaerobic and biofilm conditions were significantly greater than the one seen in the aerobic condition alone (Figure 3.6B). The oxidative phosphorylation pathway was more prominent in aerobic, anaerobic and biofilm conditions during the presence of AMK. MAB Biofilm increases glycerophospholipid metabolism and fatty acid biosynthesis in the presence of AMK. Pyruvate metabolism, glycolysis/gluconeogenesis, arginine, proline, alanine, aspartate, and glutamate metabolism increased in aerobic conditions due to AMK. We also identified nine metabolic pathways expressed under aerobic condition, seven under anaerobic condition and four under biofilm condition when treated with LNZ (Figure

3.6C). In the presence of LNZ, the oxidative phosphorylation pathway was upregulated in aerobic, anaerobic and biofilm conditions. MAB Biofilm increases glycerophospholipid metabolism in the presence of LNZ. LNZ increased ABC transporters, butanoate metabolism, and proteasome metabolism significantly in anaerobic conditions. Glycolysis/gluconeogenesis, pyruvate metabolism, arginine and proline metabolism, non-homologous end-joining and atrazine degradation increased in aerobic conditions due to LNZ.

***M. abscessus* and *M. avium* common metabolic pathways expressed under different environmental conditions and in the presence of antibiotics in aerobic conditions:** Previously we identified changes in *M. avium* proteomics expressed upon exposure to conditions that the pathogen encountered in the lung of human. We investigated *M. avium* response to amikacin and clarithromycin in aerobic conditions. We compared *M. abscessus* and *M. avium* proteomic response in anaerobic and biofilm condition. It was observed that in *M. avium*, 409 and 603 proteins were upregulated in anaerobic and biofilm conditions, while in *M. abscessus* 551 and 866 proteins were upregulated. The common proteins were used to identify their related metabolic pathways. It was observed that twenty pathways are commonly expressed under anaerobic conditions and nine pathways commonly expressed under biofilm condition, in both species (Figure 3.7A and 3.7B). Among them, five are common in both anaerobic and biofilm conditions. Those common pathways are oxidative phosphorylation, nitrogen metabolism, biosynthesis of secondary metabolites, peptidoglycan biosynthesis, and glyoxylate dicarboxylate metabolism.

In aerobic condition, proteomic analysis of *M. avium* treated with amikacin and clarithromycin 263 and 379 proteins were upregulated. Similarly, Proteomic analysis of *M. avium* treated with AMK and LNZ 587 and 755 proteins were upregulated. We compared upregulated proteins in both *M. avium* and *M. abscessus* in response to antibiotics and found that eleven metabolic pathways were common in both species (Figure 3.7C).

To enhance MAH and MAB survival during anaerobic biofilm and antibiotic treatment conditions, both bacterial species upregulate Peptidoglycan biosynthesis (Figure 3.8A). The change of cell wall structure and hydrophobic properties of the cell wall make a new permeability barrier that increase tolerance against stressful environmental conditions. In our study several genes are upregulated in both species which all are enzymes to make more peptidoglycan. Both AMH and MAB upregulates Pantothenate and CoA biosynthesis related enzymes to produce more coenzyme A (CoA) (Figure 3.8B).

Discussion

The *M. abscessus* subsp. *abscessus* (MAB) pulmonary disease treatment involves the combination of a number of antibiotics (amikacin, cefoxitin, linezolid, and others) until human sputum samples are negative for MAB [2]. To achieve MAB free sputum usually required 18-24 months of treatment with a minimum of three antibiotics [17][18]. Treatment of MAB is challenging because of the requirement of multidrug treatment for a long period of time, increasing the chances of the development of drug resistance. Macrolide regimen usually failed in pulmonary MAB isolates because of the presence of the erythromycin ribosome methyltransferase (erm) (41) gene [19]. The prolonged treatment with multiple drugs also induces toxicity in patients with decrease in compliance. Currently, there is no pipeline of the effective compound being developed to improve treatment against MAB.

One of the main challenges and perhaps a reason for current drug regimens failure is the various environmental conditions faced by the bacterium inside a human host. MAB inside a human host underwent phenotypic changes that can lead to drug tolerance. MAB disease progression is similar to that of *M. tuberculosis*, as the disease evolves MAB also live inside granuloma and experience low oxygen level (anaerobic conditions) [20]. MAB can also form biofilm inside human lung [21]. MAB in granuloma and biofilm conditioned remain in a non-replicating state characterized by low metabolic activity leads to antimicrobials tolerance. The mechanism of MAB to survive inside the human lung in either biofilm or anaerobic granuloma and MAB tolerance against antimicrobials has not been established. Previously, actively growing metabolically active replicating MAB was targeted to screen drug activity against MAB [10]. Our study describes that the proteomic response of MAB in aerobic, anaerobic, biofilm conditions as well as the proteomic response to currently used antibiotics when mapped, demonstrates how MAB in dormant non-replicating stage survives both in the absence or in the presence of antibiotics. With the change of phenotype and during exposure to bactericidal compounds, MAB upregulates and downregulates the synthesis of many enzymes associated with the pathways some of them associated with prolonging bacterial survival.

MAB in both anaerobic and biofilm conditions upregulates ten common metabolic pathways. In low oxygen conditions mycobacterium lower their ATP synthesis. The data suggest that MAB has increased levels of citrate cycle (TCA cycle), oxidative phosphorylation and glyoxylate dicarboxylate metabolism. In *M. tb,* it has been also shown a remodeling of their TCA cycle and increase glyoxylate shunt to support glycolytic and fatty acid carbon sources during hypoxia. *M. tb* increases succinate production through the TCA cycle and glyoxylate shunt to maintain membrane potentials, ATP synthesis. Succinate also serves as a substrate for SDH (succinate dehydrogenase) enzyme to synthesize ATP through oxidative phosphorylation in low O2 conditions [22].

We found that MAB increases glyoxylate and dicarboxylate metabolism in both anaerobic and biofilm conditions to maintain their carbon requirement. In *M. tb*, *Saccharomyces cerevisiae* and *Candida albicans*, differ in their outcome inside the nutrient-deprived macrophage. Their initial response is similar and all three induce glyoxylate cycle to fulfill cellular carbon requirement [23].

In MAB the nitrogen metabolism pathway-related enzymes were upregulated in both anaerobic and biofilm conditions. Further understanding of MAB nitrogen metabolism might provide new clues about innovative therapy. *M.tb, for example,* uses nitrites reducing to ammonium, which contributes to nitrogen assimilation increasing resistance against hypoxia [24]. In the absence of oxygen, *Pseudomonas aeruginosa* uses nitrate or nitrite for the respiration [25]. This indicates that nitrogen metabolism in MAB may be crucial to surviving in anaerobic condition.

From the transcriptional profiling study and proteomic experiment of *Neisseria gonorrhoeae* biofilm, researchers have described 13 KEGG pathways more expressed in biofilms. Among them, microbial metabolism in diverse environments, oxidative phosphorylation, pyruvate metabolism, glycolysis/gluconeogenesis, and citrate cycle (TCA cycle) are common metabolic pathways between *N. gonorrhoeae* and MAB are highly upregulated in both bacterial biofilms [26].

Bacteria within MAB biofilm face anaerobic condition. Our result indicates that MAB in biofilm and in anaerobic condition induces a central metabolic shifting that prolongs

their survival in stressful conditions. MAB anaerobic and biofilm condition upregulates the expression of 19 and 10 enzymes respectively, of pyruvate metabolism. *Actinobacillus pleuropneumoniae,* a respiratory pathogen, increased their protein involved in glycolysis and pyruvate metabolism after a shift to an anaerobic environment [27]. In the deeper layer of *Staphylococcus aureus* biofilm where the oxygen level is low, pyruvate metabolism-related enzymes are upregulated to maintain biofilm [28]. The opportunistic pathogen *Pseudomonas aeruginosa* upregulates pyruvate metabolizing enzyme to survival under anaerobic conditions [29].

Comparing two NTM *M. avium* and MAB to understand their proteome remodeling under anaerobic and biofilm conditions, and following exposure to bactericidal concentrations of active antimicrobials, we identified common metabolic pathways that are upregulated under environmental stresses but also expressed upon exposure to antibiotics.

This study establishes global changes in the synthesis of many enzymes promoting the shift in bacterial metabolic state and enhancing their persistence within a different environment. We found 19 and 9 metabolic pathways are prominent in both bacterial species in anaerobic and biofilm conditions, respectively. In *M. avium* and MAB anaerobic conditions Oxidative phosphorylation, Citrate cycle (TCA cycle), Glycolysis / Gluconeogenesis, Glyoxylate and dicarboxylate metabolism, Nitrogen metabolism, Peptidoglycan biosynthesis, Glycerophospholipid metabolism, Glycerolipid metabolism, and some others central metabolism-related pathways are upregulated to enhance their survival. Similarly, both bacteria in biofilm condition express some common metabolic pathway to survive in a low nutrient level with minimum metabolism. Some exclusive pathways that are upregulated in a biofilm are Nitrogen metabolism, Peptidoglycan biosynthesis, Glyoxylate and dicarboxylate metabolism, Histidine metabolism, Fatty acid metabolism, Fatty acid biosynthesis, and Pantothenate and CoA biosynthesis.

Figures

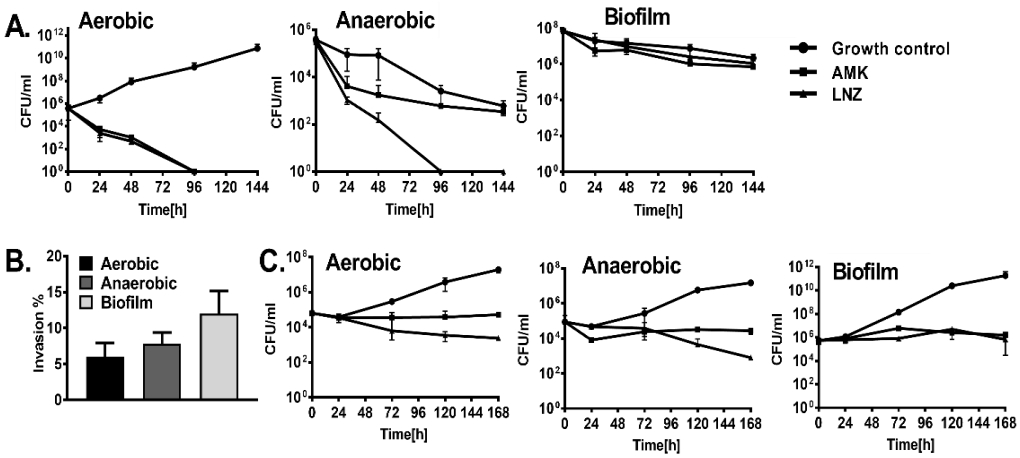

Figure 3.1: MAB killing dynamics in vitro and in macrophages. (A) MAB 19977 time-kill curves of bactericidal concentrations of AMK and LNZ show bacterial CFUs over 6 days in aerobic, anaerobic and biofilm conditions. Antimicrobials were added to the 7H9 Middlebrook liquid medium at time zero and bacterial CFUs were compared with the growth control without the drug treatment. (B) MAB 19977 invasion rates in THP-1 macrophages. Bacteria of the biofilm phenotypes had increased uptake by THP-1 cells when compared to MAB of the aerobic and anaerobic phenotype. MAB were incubated with THP-1 cells for 2 h, extracellular bacteria were removed, and macrophages were lysed for CFU counts. The percentage of invasion was established by calculating the number of bacteria (from inoculum) that entered host cells during 2h infection. (C) MAB 19977 survival rates in THP-1 macrophages. THP-1 monolayers were infected with bacteria of the aerobic, anaerobic or biofilm phenotype and killing dynamics were recorded over 7 days during AMK or LNZ treatment. Bactericidal concentrations of antimicrobials were added to the tissue culture after 2 h infection and then every alternate day. Growth control without drug treatment is also shown.

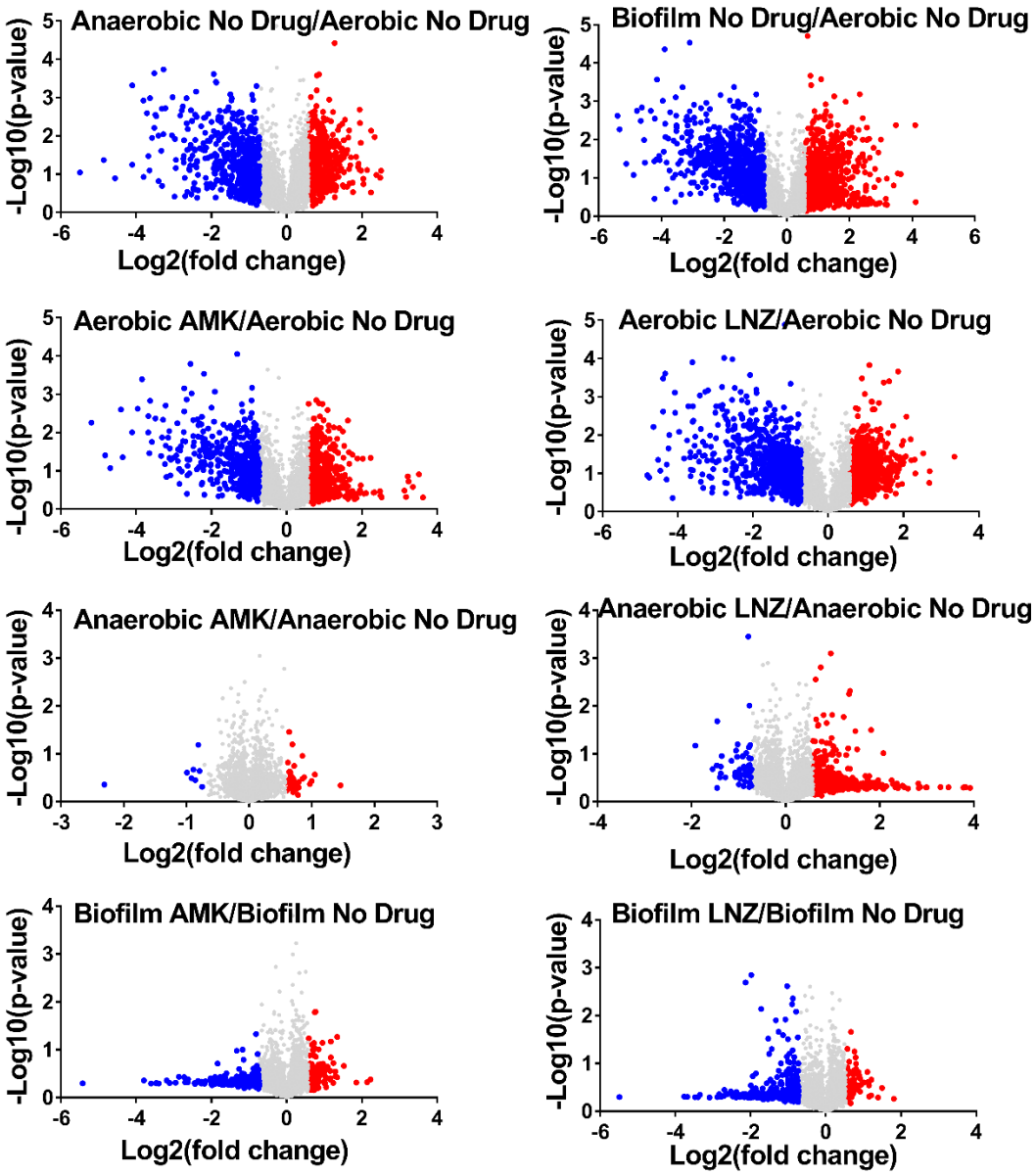

Figure 3.2: Volcano plots showing proteins that are induced or repressed. Proteins with upregulation ≥1.5 fold in red and with downregulation ≥1.5 in blue; each dot is one protein. The volcano plot shows the log2-fold changes in gene expression induced by anaerobic and biofilm conditions as compared with aerobic control. The volcano plot also shows the log2-fold changes in gene expression induced by AMK and LNZ after 24-hour exposure to aerobic, anaerobic and biofilm phenotypes. Each condition is compared with the corresponding condition with no drug.

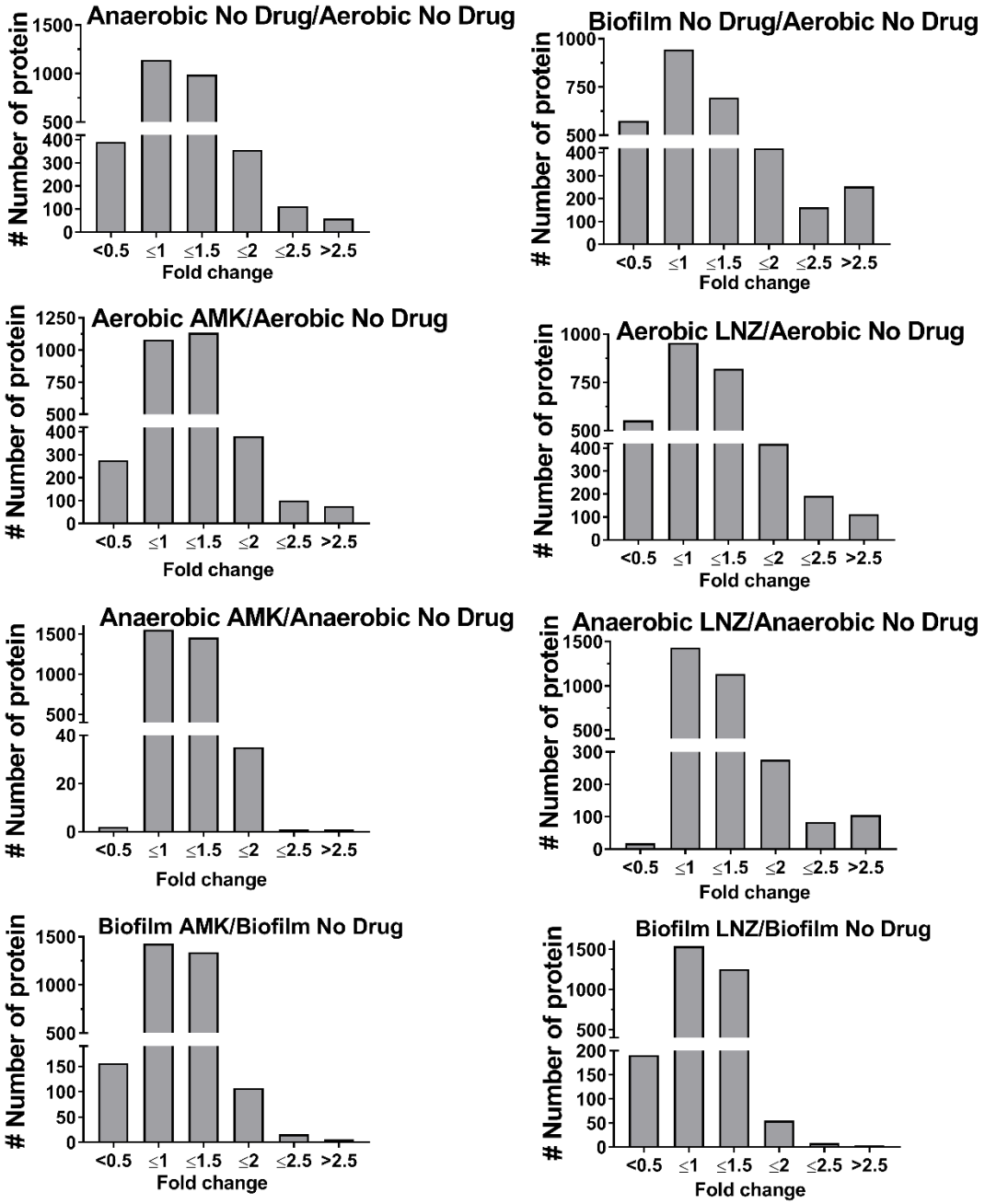

Figure 3.3: Fold changes of differentially expressed MAB proteins. The histograms show the distributions of fold changes of differentially expressed proteins in anaerobic and biofilm conditions with and without AMK and LNZ treatments.

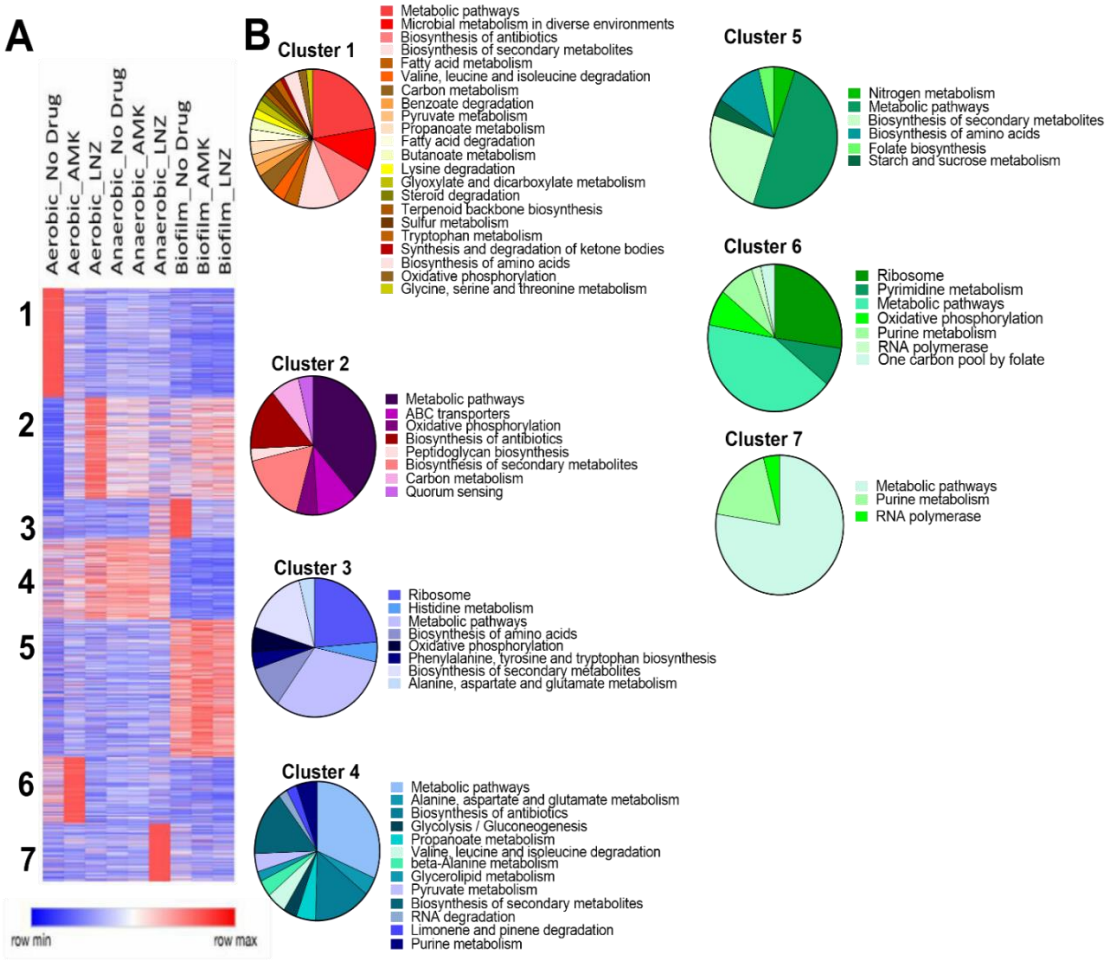

Figure 3.4: The heatmap and clustering analysis for metabolic pathways. (A) Heatmap of K-means clustering has identified groups of proteins with various expression in different treatment groups. The heat map color codes reflect a change. K-means clustering was performed for 3,722 protein-coding genes across all studied groups (adjusted p-value < 0.05). The model-based optimal number of K = 7 was determined. (B) Seven Pie charts present the KEGG enrichment analysis for metabolic pathways and correspond to 7 clusters.

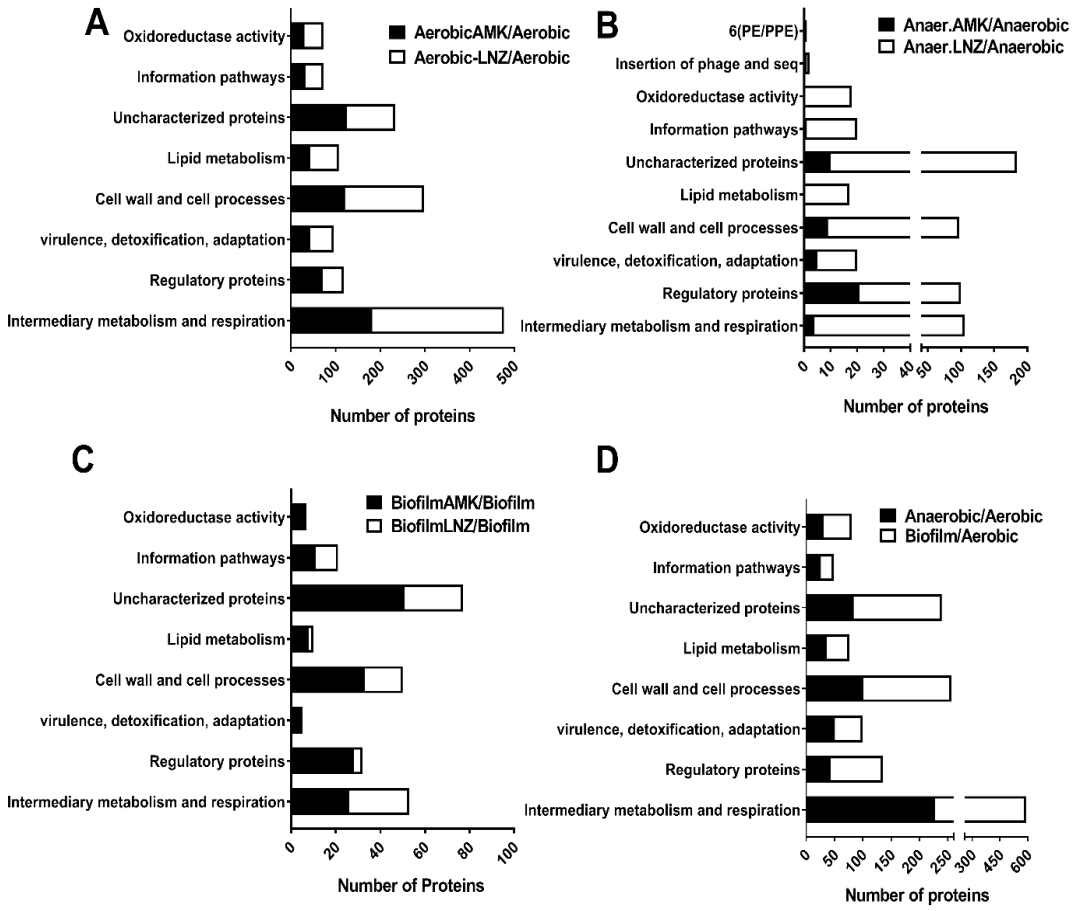

Figure 3.5: Functional classification of MAB upregulated proteins into categories was done by finding the protein homologs of H37Rv strain of Mycobacterium tuberculosis and using the functional categorization available on TubercuList webserver of Institute Pasteur or based on predicted or known function for those MAB proteins that do not match to any proteins of H37Rv strain. The histogram shows a number of proteins belonging to each functional category.

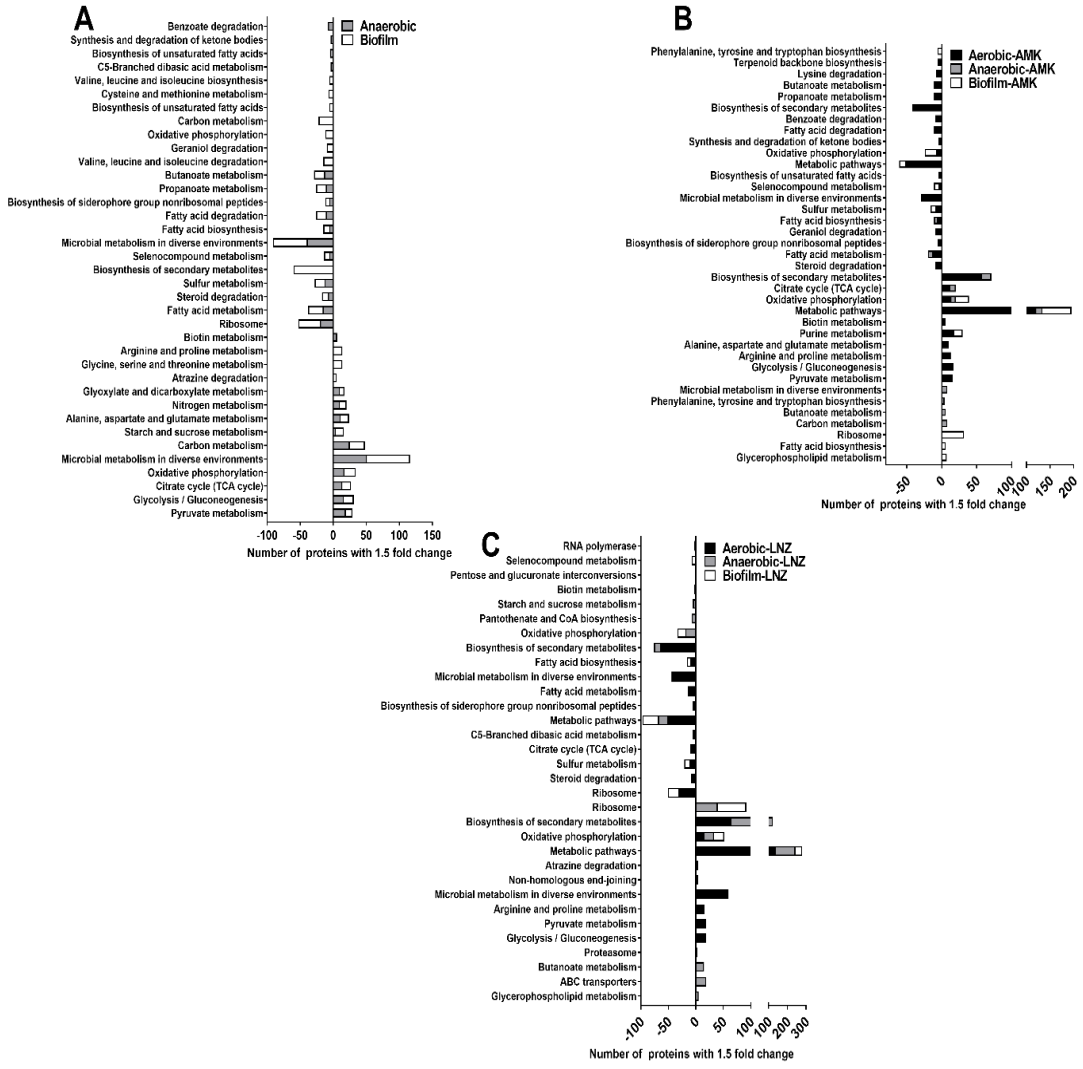

Figure 3.6: MAB metabolic pathway enrichment. Proteins are grouped based on the KEGG pathway database for upregulated and downregulated proteins in (A) anaerobic and biofilm, (B) AMK treatment aerobic, anaerobic and biofilm, and (C) LNZ treatment aerobic, anaerobic and biofilm groups.

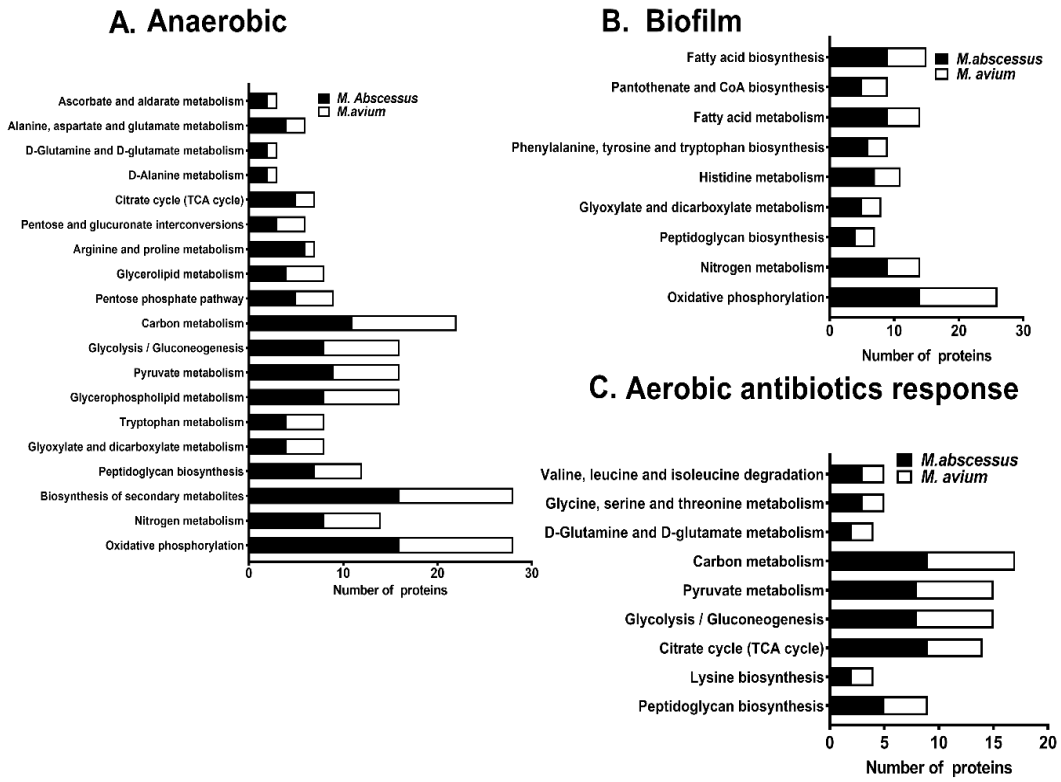

Figure 3.7: MAB and *M. avium* metabolic pathway enrichment. *M. abscessus* and *M. avium* Proteins are matched based on their amino acid sequence grouped into different metabolic pathways based on the KEGG pathway database for upregulated proteins in (A) Anaerobic conditions, (B) Biofilm conditions and (C) *M. abscessus* treated with AMK and LNZ separately and *M. avium* treated with AMK and CLA separately in aerobic conditions.

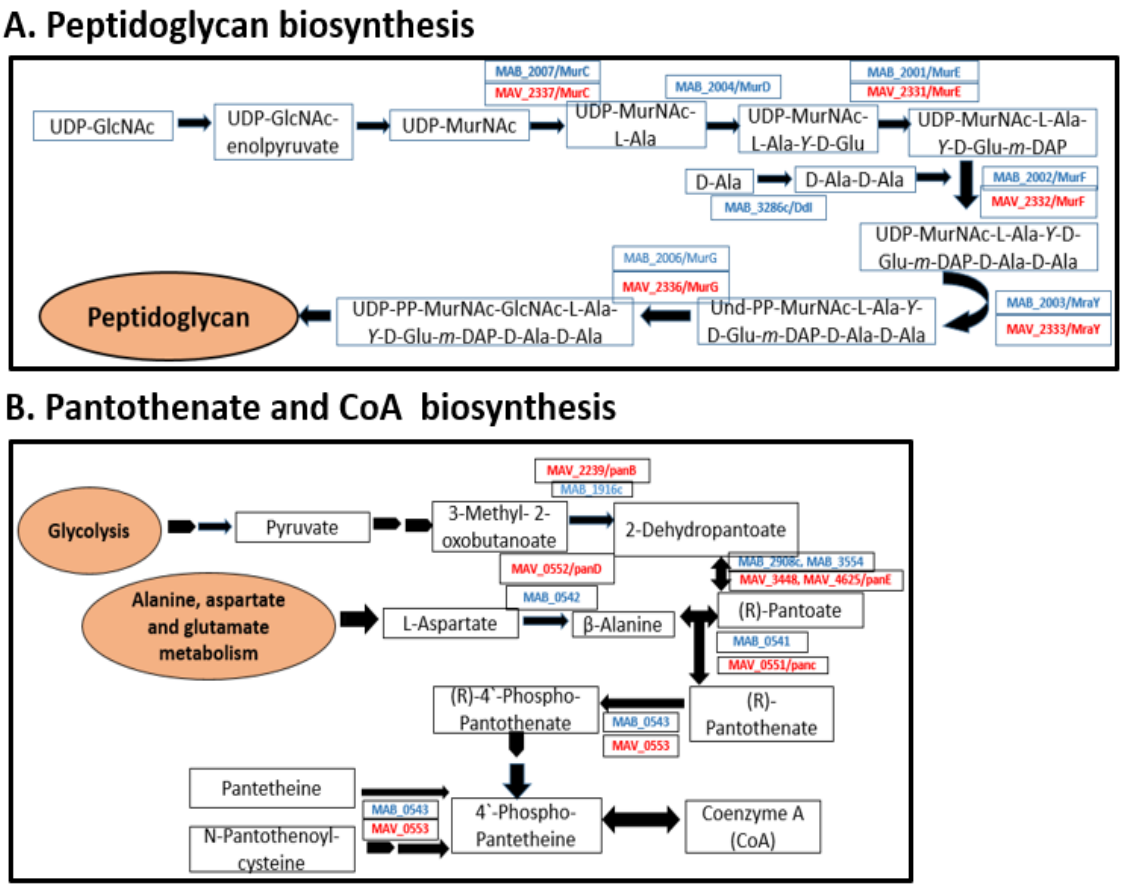

Figure 3.8: Upregulated common metabolic pathways of MAH and MAB in anaerobic and biofilm conditions. MAH Bacterial proteins synthesized are presented in red, MAB Bacterial proteins synthesized are presented in blue.

References:

[1] B. Petrini, “Mycobacterium abscessus : an emerging rapid-growing potential pathogen,” APMIS., Vol.114, Issue 5 May 2006, Pages 319-328.

[2] M. R. Lee, W. H. Sheng, C. C. Hung, C. J. Yu, L. N. Lee, and P. R. Hsueh, “Mycobacterium abscessus complex infections in humans,” *Emerg. Infect. Dis.*, vol. 21, no. 9, pp. 1638–1646, 2015.

[3] W. Koh *et al.*, “Mycobacterial Characteristics and Treatment Outcomes in Mycobacterium abscessus Lung Disease,” vol. 64, no. 41, pp. 309–316, 2017.

[4] Rachel M. Thomson “Changing Epidemiology of Pulmonary Nontuberculous Mycobacteria Infections”, Emerg Infect Dis. 2010 Oct; 16(10): 1576–1583.

[5] J. E. Stout, W. Koh, and W. Wai, “International Journal of Infectious Diseases Update on pulmonary disease due to non-tuberculous mycobacteria,” *Int. J. Infect. Dis.*, vol. 45, pp. 123–134, 2016.

[6] R. Nessar, E. Cambau, J. M. Reyrat, A. Murray, and B. Gicquel, “Mycobacterium abscessus : a new antibiotic nightmare,” J Antimicrob Chemother. 2012 Apr;67(4):810-8.

[7] R. Greendyke and T. F. Byrd, “Differential Antibiotic Susceptibility of Mycobacterium abscessus Variants in Biofilms and Macrophages Compared to That of Planktonic Bacteria □,” vol. 52, no. 6, pp. 2019–2026, 2019.

[8] B. Dickinson, M. Systems, and F. Europe, “Chronic pulmonary disease with Mycobacterium abscessus complex is a biofilm infection,” Eur Respir J. 2015 Dec;46(6):1823-6.

[9] J. P. Sarathy, L. E. Via, D. Weiner, L. Blanc, H. Boshoff, and E. A. Eugenin, “cross Extreme Drug Tolerance of Mycobacterium tuberculosis in Caseum ,” vol. 62, no. 2, pp. 1–11, 2018.

[10] R. L. Leistikow, R. A. Morton, I. L. Bartek, I. Frimpong, K. Wagner, and M. I. Voskuil, “The Mycobacterium tuberculosis DosR Regulon Assists in Metabolic Homeostasis and Enables Rapid Recovery from Nonrespiring Dormancy □ †,” vol. 192, no. 6, pp. 1662–1670, 2010.

[11] M. Wu, D. B. Aziz, V. Dartois, and T. Dick, “NTM drug discovery : status, gaps and the way forward,” vol. 23, no. 8, 2018.

[12] B. J. Berube *et al.*, “Novel Screen to Assess Bactericidal Activity of Compounds Against Non-replicating Mycobacterium abscessus,” vol. 9, no. October, pp. 1–8, 2018.

[13] S. Ager, “Clinical update on linezolid in the treatment of Gram-positive bacterial infections,” Infect Drug Resist. 2012;5:87-102.

[14] A. Z. Bialvaei, M. Rahbar, M. Yousefi, M. Asgharzadeh, and H. S. Kafil, “Linezolid: a promising option in the treatment of Gram-positives,” J Antimicrob Chemother. 2017 Feb;72(2):354-364.

[15] H. Choi *et al.*, “Linezolid for Treatment of Chronic Extensively Drug-Resistant Tuberculosis,” N Engl J Med. 2012 Oct 18;367(16):1508-18.

[16] G. F. Schecter, C. Scott, L. True, A. Raftery, J. Flood, and S. Mase, “Linezolid in the Treatment of Multidrug-Resistant Tuberculosis,” vol. 94804, pp. 49–55, 2010.

[17] J. Killingley, R. W. Wilson, D. S. York, and S. Shepherd, “Macrolide / Azalide Therapy for Nodular / Bronchiectatic Mycobacterium avium Complex Lung Disease,” Chest. 2014 Aug;146(2):276-282.

[18] H. Choi, S. Kim, H. Kim, J. Huh, and C. Ki, “Clinical Characteristics and Treatment Outcomes of Patients with Acquired Macrolide-Resistant Mycobacterium abscessus Lung Disease,” vol. 61, no. 10, pp. 1–10, 2017.

[19] S. Bastian *et al.*, “Assessment of Clarithromycin Susceptibility in Strains Belonging to the Mycobacterium abscessus Group by erm (41) and rrl Sequencing □,” vol. 55, no. 2, pp. 775–781, 2011.

[20] L. G. Wayne and L. G. Hayes, “An In Vitro Model for Sequential Study of Shiftdown of Mycobacterium tuberculosis through Two Stages of Nonreplicating Persistence,” vol. 64, no. 6, pp. 2062–2069, 1996.

[21] G. Rodríguez-sevilla *et al.*, “International Journal of Medical Microbiology Non-Tuberculous Mycobacteria multispecies biofilms in cystic fibrosis : development

of an in vitro Mycobacterium abscessus and Pseudomonas aeruginosa dual species biofilm model," *Int. J. Med. Microbiol.*, vol. 308, no. 3, pp. 413–423, 2018.

[22] H. Eoh and K. Y. Rhee, "Multifunctional essentiality of succinate metabolism in adaptation to hypoxia in Mycobacterium tuberculosis," *Proc. Natl. Acad. Sci.*, vol. 110, no. 16, pp. 6554–6559, 2013.

[23] M. C. Lorenz and G. R. Fink, "MINIREVIEW Life and Death in a Macrophage : Role of the Glyoxylate Cycle in Virulence," vol. 1, no. 5, pp. 657–662, 2002.

[24] A. Gouzy, Y. Poquet, and O. Neyrolles, "Nitrogen metabolism in Mycobacterium tuberculosis physiology and virulence" *Nat. Publ. Gr.*, vol. 12, no. 11, pp. 729–737, 2014.

[25] M. Schobert and D. Jahn, "International Journal of Medical Microbiology Anaerobic physiology of Pseudomonas aeruginosa in the cystic fibrosis lung," *Int. J. Med. Microbiol.*, vol. 300, no. 8, pp. 549–556, 2010.

[26] Phillips NJ1, Steichen CT, Schilling B, Post DM, Niles RK, Bair TB, Falsetta ML, Apicella MA, Gibson BW., "Proteomic Analysis of Neisseria gonorrhoeae Biofilms Shows Shift to Anaerobic Respiration and Changes in Nutrient Transport and Outer membrane Proteins," PLoS One. 2012;7(6):e38303.

[27] L. Li, J. Zhu, K. Yang, and Z. Xu, "Changes in Gene Expression of Actinobacillus pleuropneumoniae in Response to Anaerobic Stress Reveal Induction of Central Metabolism and Biofilm Formation §," vol. 52, no. 6, pp. 473–474, 2014.

[28] M. Leibig, M. Liebeke, D. Mader, M. Lalk, A. Peschel, and F. Go, "Pyruvate Formate-Lyase Acts as a Formate Supplier for Metabolic Processes during Anaerobiosis in Staphylococcus aureus □," vol. 193, no. 4, pp. 952–962, 2011.

[29] M. Eschbach, K. Schreiber, K. Trunk, J. Buer, D. Jahn, and M. Schobert, "Long-Term Anaerobic Survival of the Opportunistic Pathogen Pseudomonas aeruginosa via Pyruvate Fermentation," vol. 186, no. 14, pp. 4596–4604, 2004.

Chapter 4: Discussion and Conclusions

Overview

Mycobacterium avium subsp. *hominissuis* (MAH) and *Mycobacterium abscessus* subs. *abscessus* (MAB) two are the major causative agent of nontuberculous mycobacteriosis, the incidence of which is increasing in industrialized countries. MAH and MAB both are intracellular pathogens associated with disseminated infection in immunocompromised patients such as patients with HIV/AIDS. They mainly infect individuals with pre-existing chronic lung diseases, such as cystic fibrosis, bronchiectasis, and emphysema.

Mycobacteria changes their physiological, metabolic and replication dynamics in the host environment becomes more persistence and drug tolerant. Mycobacteria in unfavorable environmental conditions such as in low oxygen, low nutrient conditions maintain the non-replicate state of infection by expressing and synthesizing specific sets of proteins. In the same time, they repress certain sets of proteins to survive long-term. These phenotypic changes make current antimicrobials ineffective.

Mycobacteria form biofilm in the human respiratory tract after infection. Biofilm infections are much more drug resistance. Bacteria switch their phenotypic stages into a slower growth rate, which is one of the reasons for drug resistance. Slower growth rate reduces the antibiotic efficiency of agents active on replicating microorganisms. We also know that the mycobacterial infection makes granuloma where bacteria undergo a metabolic shift from the high oxygen environment to a region of low oxygen tension in order to survive and function effectively within the tissue spaces. This metabolic shift also interferes with antimicrobial drug treatment. Overall, metabolic shifting promotes bacteria to adopt a behavior are called “persisters”.

To kill MAH and MAB rapidly in low metabolic state, a rational therapy needs to be developed. Our strategy was to identify global proteomic remodeling of MAH and MAB within the biofilm and anaerobic conditions of the host with and without antibiotic treatments. Next, we wanted to determine what bacterial metabolic pathways were significantly associated with the MAH tolerant/persistent phenotype.

We investigated the relative protein quantitative analysis of MAH and MAB proteome under aerobic, anaerobic and biofilm conditions with and without exposure to antimicrobials using Tandem Mass Tag Mass Spectrometry approach. Our study found several synthesized and repressed proteins within different environmental stresses with or without bactericidal concentrations of antibiotics.

The phenotypic changes of mycobacteria in anaerobic and biofilm conditions have an impact on the antibiotics killing ability and host defense mechanisms. Our findings added important information about what metabolic pathway they use in different host environments and antimicrobial treatments.

Optimizing protocols

This was my first experience with cell tissue culture and there was lots of trial and error. I needed to have a strong sense of human THP-1 cell line (TIB-202) growth patterns as well as seeding plates, flasks, and passaging the cells. Every procedure related to tissue culture demands a high level of sterile technique. When performing the macrophage uptake and survival assays in the presence of antibiotics, I had to learn how to generate consistent multiplicities of infection (MOIs). I used a multiplicity of infection (MOI) of 10 and 1 for macrophage infection with MAH 104 and MAB 19977, respectively. *M. abscessus* is rapidly growing bacteria, if I use more than one MOIs, MAB will disrupt THP-1 cells within 3 days. A consistency and close to accurate MOIs helps to get accurate CFU readouts. It was very difficult to get a perfect MOI for MAB, as they are very clumpy. I did a syringe/ needle passage for at least seven times (up and down). Needle passage allowed me to disrupt MAB clumps. I got a very nice individual labeled bacterium under microscopy. To get rid of MAB extracellular bacteria, I washed infected macrophage more than five times with HBSS, treated the cells with 400μg/ml amikacin for 30min and looked under microscopy to make sure that there are no extracellular bacteria.

Another important step was sample preparation for proteomic sequencing from aerobic, anaerobic and biofilm bacterial phenotype with or without antibiotics. First, I started

with a small amount of bacteria and got a trivial amount of protein. I adapted a small modification to this protocol; I used several 25cm^2 tissue culture flasks instead of plates to form a biofilm. Then I measured protein concentrations using the Thermo Scientific NanoDrop machine and got a sufficient amount of protein to perform proteomic sequencing.

After TMT Mass Spectrometric sequencing for samples at 24 h time point and, overall, 4,000 proteins were identified across all experimental and control groups for MAH and MAB separately. We noticed in MAH anaerobic and biofilm conditions resulted in upregulation of 409 and 603 proteins, 522 and 585 proteins were downregulated when compared to MAH of aerobic condition. Proteome analysis of MAH treated with either AMK or CLA for 24 h some proteins were more expressed and some were downregulated in aerobic, anaerobic and biofilm conditions. Next, we wanted to determine what bacterial metabolic pathways were significantly associated with the MAH biofilm and anaerobic conditions with or without antibiotics.

Kyoto Encyclopedia of Genes and Genomes (KEGG), STRING (protein-protein interaction network), BioCyc pathway/genome database collection and other bioinformatics analysis tools have a database for *Mycobacterium avium* Subs *hominissuis*. When I tried to put multiple protein name, gene ID or multiple MAH accession number all of the above-mentioned bioinformatics tools repudiates to generate metabolic pathways related to multiple expressed or repressed proteins. To solve this issue I used a free software called R for statistical computing. Although R has a command line interface called RStudio. A package called KEGGgraph was used to integrate pathway data that have been identified and described.

We noticed in MAB anaerobic and biofilm conditions resulted in upregulation of 551 and 866 proteins, 556 and 743 proteins were downregulated when compared to MAB of aerobic condition. Proteome analysis of MAB treated with either AMK or LNZ for 24 h some proteins were more expressed and some were downregulated in aerobic, anaerobic and biofilm conditions. To determine what bacterial metabolic pathways were significantly associated with the MAB biofilm and anaerobic conditions with or without antibiotics, I used a proteome-scale interaction network of proteins in *M. abscessus* was derived from the STRING version 11.0 database. All expressed or

repressed protein ID separately were archived for network analysis. STRING11 was used to construct a network of interaction. I downloaded and used all pathway enrichment analysis based on KEGG. I used all-important pathways based on low p-value (<0.05) and low false discovery rates for further analysis.

***Mycobacterium avium* subs *homonisuis* and *Mycobacterium abscessus* subs. *abscessus* common metabolic pathways expressed under environmental conditions:** our study investigated global proteome changes in the synthesis of many enzymes promoting the shift in the bacterial metabolic state in biofilm and anaerobic conditions. Shifting of metabolic pathway enhances bacterial persistence within the different condition and promotes antibiotic tolerance as well.

We found that both in MAH and MAB bacterial species, a total of 19 and 9 metabolic pathways are prominent in anaerobic and biofilm conditions, respectively. To enhance anaerobic survival, both bacterial species upregulate Oxidative phosphorylation, Citrate cycle (TCA cycle), Glycolysis / Gluconeogenesis, Glyoxylate and dicarboxylate metabolism, Nitrogen metabolism, Peptidoglycan biosynthesis, Glycerophospholipid metabolism, Glycerolipid metabolism, and some others central metabolism related pathways.

The glyoxylate cycle has a central role in the metabolism of pathogenic mycobacteria in the non-growing stage. Mycobacteria becomes quiescent by either oxygen depletion or nutrient depletion and use enzymes associated with the glyoxylate shunt to maintain their intracellular ATP level. One of the glyoxylate cycle enzyme called isocitrate lyase has been exploited for the development of additional anti-TB therapy. In anaerobic condition, *M. tb* uses glycine dehydrogenase to catalyze the reductive amination of glyoxylate. The glyoxylate synthesis provides a substrate for the regeneration of NAD from NADH in oxygen-depleted conditions.

Both MAH and MAB increase nitrogen metabolism in anaerobic conditions. We identified nitrate transporter, nitrite transporter and nitrite reductase enzymes of MAH and MAB was highly upregulated under anaerobic and biofilm conditions. In mycobacteria, nitrate reduction pathways play a vital role during the survival in

anaerobic condition. If we can target some enzymes involved in nitrogen metabolism pathway may help in developing novel drugs.

In anaerobic condition, MAH and MAB both increase Peptidoglycan biosynthesis, Glycerophospholipid metabolism and Glycerolipid metabolism. *M. tuberculosis* can survive several months in presence of antibiotic treatment by changing their peptidoglycan network.

To enhance MAH and MAB survival in biofilm conditions, both bacterial species upregulate Nitrogen metabolism, Peptidoglycan biosynthesis, Glyoxylate and dicarboxylate metabolism, Histidine metabolism, Fatty acid metabolism, Fatty acid biosynthesis, and Pantothenate and CoA biosynthesis pathway.

Both MAH and MAB increase histidine metabolism pathways to promote more biofilm formation. In literature review, we found that *Acinetobacter baumannii* and *Staphylococcus xylosus* also increase their histidine metabolism for biofilm formation. Histidine auxotroph strains of *M. tuberculosis* are unable to survive during prolonged starvation. Upregulation of several histidine metabolism related enzymes of MAH and MAB raises the possibility that histidine metabolism may play an important role during biofilm formation.

Pantothenate and CoA biosynthesis pathways are upregulated in MAH and MAB biofilm. MAH increases production of Pantothenate and CoA biosynthesis related enzymes named (panB/MAV_2239), (panC/MAV_0551), (panD/MAV_0552), (MAV_0553), (panE/MAV_3448, MAV_4625). Similarly, MAB increases corresponding enzymes named (panB/MAB_1916c), (panC/MAB_0541), (panD/MAB_0542), (MAB_0543), (panE/MAB_2908c, MAB_3554) to produce more coenzyme A (CoA). CoA, a cofactor involved in tricarboxylic acid cycle, phospholipids synthesis, fatty acids synthesis and degradation. It has been observed that immunocompromised SCID mice infected with ΔpanCD knockout *M. tuberculosis* mutants, survived for more than 30 weeks longer than WT *M. tuberculosis* infected mice. Since MAH and MAB both share many traits with *M. tuberculosis* during biofilm formation, it is tempting to hypothesize that some of the genes found in our proteome study could be involved with bacterial virulence.